Geoelectric structure of the Proterozoic Wopmay Orogen and adjacent terranes, Northwest Territories, Canada[1, 2]

Xianghong Wu, Ian J. Ferguson, and Alan. G. Jones

Abstract: Magnetotelluric (MT) soundings were made along a transect in northern Canada crossing the Proterozoic Wopmay Orogen, Fort Simpson basin, and adjacent parts of the Slave craton and the Nahanni terrane. The results are used to define the geoelectric structure and constrain the crustal and lithospheric structure and evolution. Across the Wopmay Orogen, geoelectric strikes at crustal depths average N34°E and are interpreted to be related to transcurrent faulting that occurred during late distal collisions at the western margin of the orogen. Weak two-dimensionality in the Fort Simpson basin is interpreted to be due to the sedimentary rocks in the basin. At longer periods, geoelectric strikes across the Wopmay Orogen rotate from ~N43°E at uppermost mantle penetration to ~N62°E at a depth of 100 km. The uppermost mantle strikes are interpreted to be due to ductile shearing linked to the transcurrent faulting in the overlying crust. The deeper strikes may be caused by shearing at the base of the present-day lithosphere. Within the Wopmay Orogen, the MT results image a conductor at the margin of the Fort Simpson and Hottah terranes interpreted to be related to the collision of these terranes. Conductive crust beneath the western margin of the Great Bear magmatic arc suggests correlative rocks of the Coronation margin extend south of the Slave craton. Lastly, decreased resistivity in the Hottah terrane at mantle depths is interpreted to be caused by the introduction of graphitic or sulphidic rocks during subduction prior to the Hottah–Slave and Fort Simpson – Hottah collisions.

Résumé : Des sondages magnétotelluriques ont été effectués le long d'une géotraverse à travers l'orogène Wopmay (Protérozoïque), le bassin de Fort Simpson et des parties adjacentes du craton des Esclaves ainsi que le terrane de Nahanni, dans le nord du Canada. Les résultats sont utilisés pour définir la structure géoélectrique et encadrer la structure et l'évolution crustale et lithosphérique. À travers l'orogène de Wopmay, les directions géoélectriques à des profondeurs crustales ont en moyenne N34ºE et elles sont interprétées comme étant reliées aux failles décrochantes qui se sont produites durant des collisions distales tardives à la limite ouest de l'orogène. Une faible double dimensionnalité dans le bassin de Fort Simpson résulterait de la présence de roches sédimentaires dans le bassin. Lors de périodes plus longues, les directions géoélectriques à travers l'orogène de Wopmay ont subi une rotation de N43ºE, à l'endroit de pénétration le plus haut dans le manteau, à N62ºE, à une profondeur de 100 km. Les directions dans la partie supérieure du manteau seraient dues à un cisaillement ductile relié aux failles décrochantes dans la croûte sus-jacente. Les directions plus profondes peuvent être causées par un cisaillement à la base de la lithosphère actuelle. À l'intérieur de l'orogène Wopmay, les résultats magnétotelluriques révèlent l'image d'un conducteur à la bordure des terranes de Fort Simpson et de Hottah; ce conducteur serait relié à la collision de ces terranes. Une croûte conductrice sous la bordure ouest de l'arc magmatique Great Bear suggère que des roches en corrélation avec la bordure Coronation s'étendent au sud du craton des Esclaves. Finalement, à des profondeurs du manteau, une résistivité moindre dans le terrane de Hottah serait causée par l'introduction de roches graphitiques ou sulfuriques durant la subduction, avant les collisions Hottah – Esclave et Fort Simpson – Hottah.

[Traduit par la Rédaction]

Received 22 March 2004. Accepted 13 April 2005. Published on the NRC Research Press Web site at http://cjes.nrc.ca on 9 September 2005.

Paper handled by Associate Editor R.M. Clowes.

X. Wu[3] and I.J. Ferguson.[4] Department of Geological Sciences, University of Manitoba, Winnipeg, MB R3T 2N2, Canada.
A.G. Jones.[5] Geological Survey of Canada, 615 Booth Street, Ottawa, ON K1A 0E9, Canada.

[1]This article is one of a selection of papers published in this Special Issue on *The Lithoprobe Slave – Northern Cordillera Lithospheric Evolution (SNORCLE) transect*.
[2]Lithoprobe Publication 1397.
[3]Present address: Offshore Hydrocarbon Mapping Inc., 12600 Exchange Drive, Suite 204, Houston, TX 77477, USA.
[4]Corresponding author (e-mail: ij_ferguson@umanitoba.ca).
[5]Present address: Dublin Institute for Advanced Studies, 5 Merrion Square, Dublin 2, Ireland.

 doi: 10.1139/E05-042 © 2005 NRC Canada

Introduction

The northwestern part of the North American continent provides a record of 4 billion years of tectonic evolution. The Canadian Lithoprobe Project is investigating this area with multidisciplinary, geoscientific studies along its Slave – Northern Cordillera Lithospheric Evolution (SNORCLE) Transect (Clowes 1997). Corridor 1 of the transect is located in the Northwest Territories, Canada. It crosses the southwestern part of the Archean Slave craton and southern part of the Proterozoic Wopmay Orogen (Fig. 1), spanning basement rocks ranging in age from Mesoarchean to Neoproterozoic. Corridor 1a is a southeastern extension of the main profile that provides a second east–west crossing of the eastern part of the Wopmay Orogen and the Great Slave Lake shear zone (GSLsz), reported recently in Wu et al. (2002).

Along parts of corridors 1 and 1a the Precambrian rocks are covered by up to 1000 m of Devonian sedimentary rocks (Fig. 1). Prior to the Lithoprobe studies the structure of these areas was interpreted using extrapolations from the exposed part of the orogen, potential-field data, and sparse drill-core intersections. Geophysical surveys done in the Lithoprobe project including seismic reflection (Cook et al. 1999), seismic refraction (Fernández Viejo and Clowes 2003), and magnetotelluric (MT) enable accurate and detailed definition of the structure of the crust and mantle lithosphere along a profile crossing the Wopmay Orogen.

In this paper, we analyse and interpret MT data collected along the western parts of corridors 1 and 1a with the primary objective of defining the geoelectric structure of the Proterozoic terranes of the Wopmay Orogen and using the results to constrain the lithospheric structure and tectonic history of the region. Large-scale electromagnetic soundings, such as the MT survey in the present study, provide images of the electrical resistivity structure of the crust and mantle lithosphere. Unlike seismic velocity and density, in which the physical response is most sensitive to the bulk properties of rocks, resistivity is particularly sensitive to certain minor constituents of rocks. A small amount of graphite or connected grains of metallic sulphides and oxides can significantly decrease the resistivity of crustal rocks by allowing metallic conduction. Saline fluids or melt can decrease crustal resistivity by allowing ionic conduction. Decreased resistivity within the mantle has been typically attributed to the presence of graphite, hydrogen, partial melt, and water (Jones 1999; Hirth et al. 2000). The sensitivity of electromagnetic methods to these geological constituents means the method can provide unique geological information that is complementary to other deep-sounding geophysical methods.

MT signals of different periods penetrate to different depths into the Earth: short-period MT signals (10^{-4}–10^{-3} s) penetrate several hundred metres into the Earth, whereas long-period signals (10^{3}–10^{4} s) typically penetrate 100 km or more into the upper mantle. The MT period range in the present study is from 10^{-4} to 10^{4} s, allowing imaging of the surface Palaeozoic sedimentary rocks, the Proterozoic crust, and the underlying lithospheric mantle.

An electromagnetic study by Camfield et al. (1989) provided information on the electrical resistivity structure of an exposed part of the Wopmay Orogen 500 km to the north of the present study area (Fig. 1). These authors undertook an electromagnetic study along a 240 km east–west profile in the Coronation margin using mainly the geomagnetic depth sounding (GDS) method. The GDS method provides excellent detection of conducting anomalies in the crust but less resolution of the exact depth and geometry of these conductors. The survey results indicated the presence of a linear conductor, here called the Northern Wopmay Conductor (NWC), crossing the profile which Camfield et al. modelled with a 50 km-wide body of thickness 1.5 km and resistivity 20 Ω·m. The conductor is spatially correlated with the graphitic pelites of the Odjick Formation, a slope-rise facies deposit. Boerner et al. (1996) suggested that the conductor may be due to the foredeep facies rocks and specifically the euxinic shale of the Fontano Formation.

Analyses of SNORCLE electromagnetic survey data from the eastern parts of corridors 1 and 1a have already provided information on a range of tectonic structures. Jones and Ferguson (2001) and Jones et al. (2001, 2003, 2005) describe analyses of data from the Slave craton. Wu et al. (2002) analysed the geoelectric response across the 1.9 Ga GSLsz and the later brittle McDonald fault (MF) that formed during collision of the Slave craton and Hearn Province. The results showed that the shear zone is characterized by a coincident resistivity high and magnetic low. Eaton et al. (2004) have compared the MT and teleseismic shear-wave splitting response across the shear zone and found that seismic anisotropy in the region of the fault zone is associated with lithospheric structure, and anisotropy within the shear zone is perturbed by crustal structures. The present study focuses on the western parts of corridors 1 and 1a.

Geological and geophysical setting

The eastern end of SNORCLE Transect corridor 1 traverses the Anton complex in the southwest part of the Archean Slave craton (Fig. 1). This complex was previously defined as a unique basement terrane but is now recognized as an integral part of a Paleoarchean to Mesoarchean basement complex of much of the Slave craton (Bleeker et al. 1999*a*, 1999*b*).

The eastern end of corridor 1a crosses the GSLsz, which is a northeast-trending dextral continental transform fault, with up to 700 km of strike-slip motion, extending along the southeast side of Great Slave Lake (Hoffman 1987; Hanmer et al. 1992). U–Pb zircon ages on syntectonic granites define a minimum duration for ductile shear of 2.03–1.95 Ga (Hoffman 1987). The MF system is a later brittle strike-slip fault system roughly coincident with the GSLsz in mapped exposures northeast of the present study area. The MF system was caused by post-collisional convergence of the Slave and Rae provinces (Ritts and Grotzinger 1994) and (or) obduction of the Wopmay Orogen to the Slave craton (Ross 2002). It accommodated some 75–125 km of strike-slip motion between 1.86 and 1.74 Ga. Due to the cover, the exact location at which corridor 1a crosses the MF is uncertain. On the basis of magnetic field patterns, Eaton and Hope (2003) interpret its position to be near the west end of Great Slave Lake, crossing the western end of corridor 1a (Fig. 1).

The 1.9–1.8 Ga Proterozoic Wopmay Orogen comprises a series of north–south-trending tectonic units (Fig. 1) and formed as microcontinents and volcanic arcs were accreted

© 2005 NRC Canada

Fig. 1. (*a*) Location of the Lithoprobe SNORCLE corridors 1, 1a, 2a, 2b, and 3 in northwestern Canada. (*b*) Tectonic elements of the northwest Canadian Shield (after Hanmer 1988). The solid circles show the location of the MT sites in corridor 1 (Cor. 1) and corridor 1a (Cor. 1a), and the black bar indicates the location of the survey by Camfield et al. (1989). The heavy broken line indicates the eastern margin of the Phanerozoic sedimentary cover. Tectonic units: BF, Bathurst fault zone; BH, Buffalo Head terrane; FS, Fort Simpson terrane; GB, Great Bear magmatic arc; GSLsz, Great Slave Lake shear zone; Ho, Hottah terrane; MF, McDonald fault system. Na, Nahanni terrane; SC, Slave craton; Ta, Talston magmatic zone; Th, Thelon magmatic zone. Geographic features: GBL, Great Bear Lake; GSL, Great Slave Lake. Electrical features: KC, Kiskatinaw Conductor; NWC, Northern Wopmay Conductor.

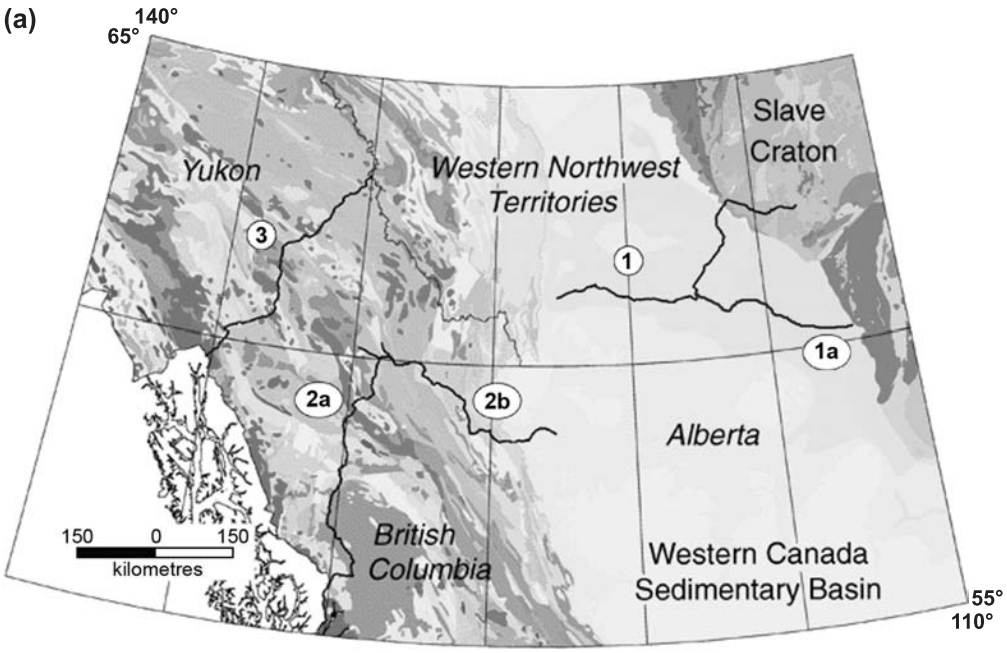

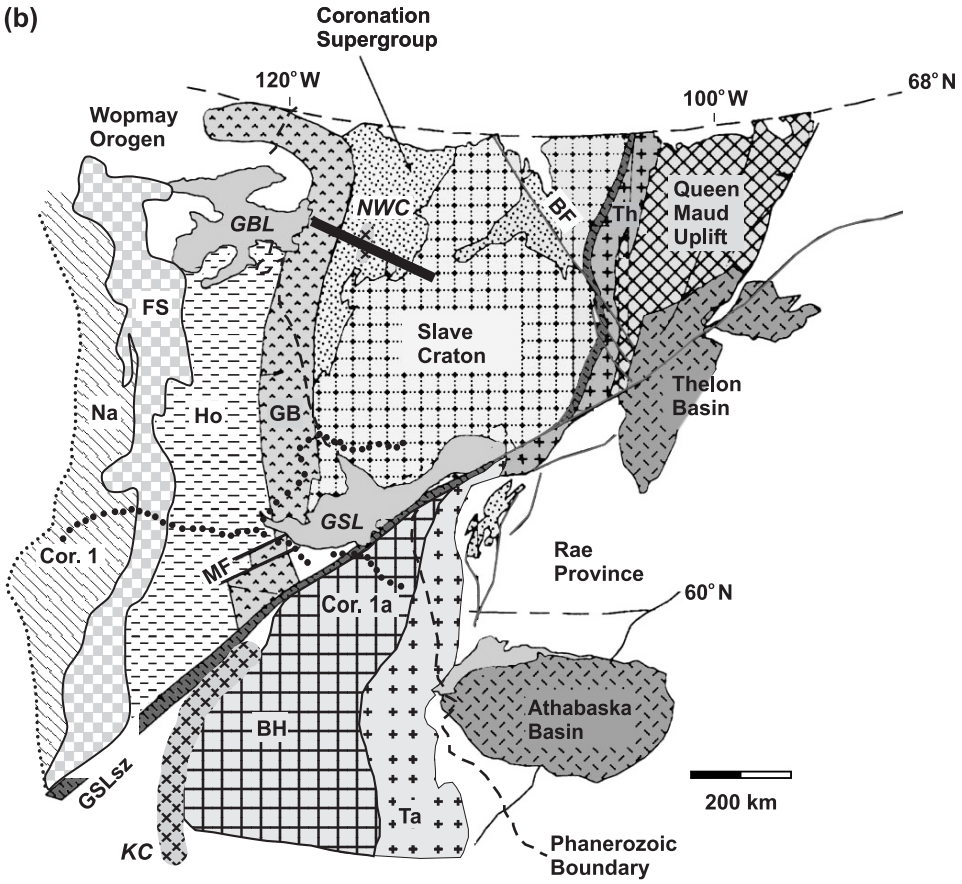

© 2005 NRC Canada

to the western margin of the Slave craton. The passive western margin of the Slave craton is recorded in the Coronation margin rocks exposed 200 km to the north of the Lithoprobe profile (Hoffman and Bowring 1984). The deposits record the transition from the opening of an ocean basin to subsequent collision of its margins.

The Hottah terrane consists of magmatic arc and associated sedimentary rocks that formed distally and to the west of the Slave craton at 1.92–1.90 Ga (Hoffman and Bowring 1984; Hildebrand et al. 1987). It is intruded by calc-alkaline plutons (1.914–1.902 Ga). The affinity of the basement on which the magmatic arc formed is uncertain, but Pb and Nd isotopic data and zircon dating suggest it was generated on cryptic 2.4–2.0 Ga crust (Housh and Bowring 1988). The formation of the Hottah arc was probably coeval with the sedimentation on the Coronation margin.

Collapse of the ocean basin off the western Slave craton occurred during the 1.90–1.86 Ga Calderan orogeny. It is interpreted to have involved an initial phase of westward-directed subduction of oceanic rocks beneath Hottah crust (Cook et al. 1999) followed by a polarity reversal and attempted eastward subduction. The Coronation margin and the Hottah magmatic arc were translated eastwards at ca. 1.885 Ga. Some of the Hottah terrane rocks were thrust over the Coronation Supergroup rocks as both were thrust over the Slave craton (Cook et al. 1999).

The Great Bear magmatic arc forms a 100 km-wide zone of volcanosedimentary sequences and plutonic rocks (Hildebrand et al. 1987). The 1.875–1.840 Ga rocks of the arc were deposited on both the Hottah terrane and deformed rocks of the Coronation margin. The magmatic arc is interpreted as the product of eastward subduction of oceanic lithosphere beneath the west of the Hottah terrane (Cook et al. 1998). Along Lithoprobe corridor 1, the Proterozoic rocks occur beneath Phanerozoic sedimentary rocks, but on the basis of aeromagnetic data the rocks of the Great Bear magmatic arc are interpreted to extend to the margin of the Anton terrane. Seismic reflection results suggest that the magmatic arc forms a thin (3.0–4.5 km thick) basin (Cook et al. 1998) overlying deformed rocks of the Hottah–Slave transition.

Rocks of the Great Bear magmatic arc were deformed by right-lateral oblique slip at 1.86–1.84 Ga (Cook et al. 1999). A subsequent phase of compression within the Great Bear – Hottah – Slave assembly is interpreted to be either the terminal collision of the Fort Simpson terrane with the Hottah terrane (Hildebrand et al. 1987) or docking of the Nahanni terrane to the west (Hoffman 1989). The deformation resulted in brittle conjugate transcurrent faulting similar to that produced by distal collisions in other orogenic belts (Hildebrand et al. 1987).

A series of lower crustal reflections beneath the eastern Great Bear magmatic arc suggests that during the Hottah collision part of the lower Wopmay crust was thrust eastwards beneath the Slave craton. The reflections define a wedge of Slave crust with its tip located at 25 km depth beneath the Great Bear magmatic arc. Cook et al. (1998) suggest the wedge formed above a detachment near the Moho that connected the deformation with structures farther to the west. A prominent mantle reflector dips eastward from the base of the crust near the Great Bear magmatic arc to a depth of ~85 km, from where it extends subhorizontally beneath the Slave craton. This reflection may define an imbrication surface that accommodated the intracrustal deformation in the Slave–Hottah collision. In this case, the surface forms an interface between Slave mantle lithosphere and underlying Wopmay mantle lithosphere (Cook et al. 1998).

The exact nature of the Wopmay crust beneath and to the east of the part of the Great Bear magmatic arc along Lithoprobe corridors 1 and 1a remains uncertain. Cook et al. (1999) compare structures in which Coronation margin sediments and Hottah crust form this crust. On the northwest side of the GSLsz, the Phanerozoic rocks are underlain by a granitic basement domain associated with a region of negative magnetic anomaly values. This crustal unit has been referred to as the Hay River terrane by Ross et al. (2000), and a single dated basement cutting from the terrane yielded a Paleoproterozoic age of 1838 ± 5 Ma (Ross et al. 2000).

The Fort Simpson terrane contains 1.845 Ga magmatic rocks (Villeneuve et al. 1991), and its terminal collision with the Hottah terrane occurred after the formation of these rocks and pre-1.710 Ga (Cook et al. 1999). Seismic reflection data reveal that the Hottah – Fort Simpson margin possesses a wedge-shaped geometry (Snyder 2000). In the upper crust, the reflectors dip to the west, and a 10 km-wide zone of strong reflectivity projects to the surface at the location of a prominent gravity high and prominent magnetic trend (the Johnny Hoe suture). This location has been interpreted to mark the suture between the Fort Simpson magmatic arc and the Hottah terrane (Hildebrand et al. 1987). The geometry suggests that the upper crust of the Fort Simpson magmatic arc was detached and thrust over a tectonic wedge. The geometry and internal characteristics of the reflectivity within the wedge are consistent with it being an accretionary complex as seen in modern convergent zones (Cook et al. 1998). Hildebrand et al. (1987) interpret magmatism within the overlying Hottah crust as being due to the subduction (or wedging) of the Hottah crust.

At greater depth the reflectors dip eastwards, suggesting the lower crust of the Fort Simpson terrane was carried into the mantle attached to the crust subducting beneath the wedge (Cook et al. 1999). Corresponding reflections can be traced to 100 km depth beneath the Great Bear magmatic arc (Cook et al. 1998). A series of reflectors overlying the dipping reflectors is interpreted as evidence of a fossil subduction zone that was isolated when active subduction migrated to the west. The geological structure of the western parts of the Fort Simpson terrane is not fully understood. Seismic reflection data image two antiformal structures at ~15–20 km depth that appear to represent structures formed during collision with the Hottah crust (Cook et al. 1999).

On the basis of seismic reflection data from Lithoprobe corridor 1 and earlier seismic results, the Fort Simpson basin formed within the Fort Simpson terrane during a period of lithospheric extension. Seismic reflection data reveal a thick sequence of west-dipping reflectors that define a west-facing monocline (Cook et al. 1999) with a base that dips westwards at 20°–30° from a depth of 3 km at the eastern end to a depth of ~24 km at the western end. The reflectors interpreted as defining the base of the basin project to the surface at a point about 50 km west of the boundary of the Fort Simpson and Hottah terranes (Cook et al. 1999).

© 2005 NRC Canada

Integration of Lithoprobe corridors 1, 2, and 3 results suggests the sedimentary rocks in the Fort Simpson basin form part of a very extensive sequence of Proterozoic rocks that extends into the middle and lower crust of the northern Cordillera (Snyder et al. 2002; Cook et al. 2004). Based on outcrop correlations, this sequence of passive margin sedimentary rocks is considered to include rocks of the 1.84–1.71 Ga Wernecke Supergroup, the 1.815–1.500 Ga Muskwa assemblage, the 1.20–0.78 Ga Mackenzie Mountain Supergroup, and the 0.80–0.54 Ga Windermere Supergroup.

The Nahanni terrane is located to the west of the Fort Simpson crust. The classification of this crust as a separate terrane was based on potential-field anomalies, as the basement does not outcrop: it is characterized by variable but mostly low-magnitude magnetic anomalies (Pilkington et al. 2000). Cook et al. (1999) suggest that the magnetic low may be associated with thinned Fort Simpson crust. Isotopic dating of rocks presumed to be derived from the Nahanni terrane in overlying units, however, has indicated younger ages, suggesting that the terrane may contain components with a different origin (Aspler et al. 2003).

Along the Lithoprobe transect the Proterozoic rocks of the Wopmay Orogen are overlain by Phanerozoic sedimentary rocks. The eastern margin of the cover is in the Great Bear magmatic arc, and the thickness of the sedimentary rocks increases from east to west, reaching a value of around 1000 m above the Fort Simpson terrane. The Phanerozoic sequence is Middle to Upper Devonian in age and consists of gently westward dipping shales, siltstones, and limestone units (Aitken 1993). The sedimentary rocks thin to around 200 m over the Bulmer Lake High, a Precambrian paleotopographic high within the Fort Simpson terrane (Law 1971; Meijer-Drees 1975). In corridor 1a, the Presqu'ile barrier separates sedimentary rocks of the Mackenzie basin in the northwest from those of the Elk Point basin in the southeast (Rhodes et al. 1984).

Magnetotelluric survey and data processing

The MT survey along Lithoprobe SNORCLE corridors 1 and 1a was undertaken in 1996 and consisted of 60 MT sites (denoted sno*xxx*) with an average site spacing of 15 km (Fig. 2). The survey was done prior to the availability of seismic reflection and refraction results for the profile and was designed to provide reconnaissance-level definition of the resistivity structure of the Wopmay Orogen and adjacent terranes. MT impedance responses were determined at each site for an eight-decade period range of 10^{-4}–10^{4} s. This period range provides resolution of the electrical structure over a depth range extending from the uppermost crust (several tens to hundreds of metres) to the deep lithospheric mantle (>100 km).

The MT instrumentation used in the survey is described in Jones et al. (2005). Corridor 1 is located at a relatively high geomagnetic latitude (66°N–69°N), and the recorded MT time series contains relatively strong geomagnetic activity, particular around local midnight, interpreted to be associated with the auroral electrojet. The nonuniform source field associated with these signals can cause appreciable bias to the MT response at periods longer than a few tens of seconds (Jones 1980; Garcia et al. 1997; Jones and Spratt 2002). The 2×2 complex MT impedance tensor, which relates the horizontal electric and magnetic fields, is the fundamental response determined from the recorded electric and magnetic field components (e.g., Vozoff 1991). Several investigations of the best method for reducing the bias in SNORCLE MT impedance data have been completed. Methods applied include the robust Jones–Jödicke weighted cascade decimation approach (method 6 in Jones et al. 1989), using both single and multiple remote-reference sites, and the Chave robust remote-reference impedance estimation approach (Chave et al. 1987; Chave and Thomson 1989). The consistency of responses obtained from recordings of two-night duration with broadband MT instrumentation and those obtained from recordings of > 1 week duration with long period instrumentation suggests that, at periods < 1000 s, the impedance estimates contain minimal bias. The final impedance estimates were determined using robust cascade decimation, with a single remote reference at periods < 20 s and multiple remote stations at longer periods (Wu 2001).

Each MT impedance tensor term can be used to estimate an apparent resistivity, a spatially averaged resistivity over the penetration depth of the signals. The phase of the impedance, the phase lead of the electric field over the magnetic field, also provides information on the underlying resistivity structure. Figure 3 illustrates an example of the apparent resistivity and phase responses from a site in corridor 1. The overall MT data quality is excellent. At some sites, reasonable data were even acquired in the high-frequency "dead band" around 10^{-3} s (Garcia and Jones 2002), albeit with lower quality. The absence of anthropogenic noise and low electric field distortion allowed determination of highly precise estimates of the MT impedance tensor in all elements for almost all sites.

Magnetotelluric responses

Geoelectric strike azimuth

The electromagnetic fields over a two-dimensional (2-D) structure, in which the resistivity structure is invariant in the geoelectric strike direction, can be separated into two independent modes. These modes involve electric current flow parallel to strike, called the transverse electric (TE) mode, and electric flow perpendicular to strike, called the transverse magnetic (TM) mode. Strike, and its period variation, is a useful parameter that can be correlated with other geological and geophysical data, e.g., Marquis et al. (1995) and Wu et al. (2002).

Geoelectric strike, and its variation with period, can be determined from the observed MT response using several methods. The most straightforward method is a rotation of the coordinate system, in which the impedance is defined to find the orientation in which the impedance is closest to a 2-D form. In the case of the phase response, the geoelectric strike is obtained by determining the coordinate system in which there is a maximum absolute difference between the estimates of the TE and TM mode phase. Electric charge accumulation on near-surface heterogeneities can distort the amplitudes of the measured MT response, so it no longer accurately represents the larger scale or regional resistivity structure. In the Groom–Bailey (GB) tensor decomposition method (Bailey and Groom 1987; Groom and Bailey 1989,

© 2005 NRC Canada

Fig. 2. Location of individual MT sites in corridors 1 and 1a. The stars show the location of MT sites in the Wopmay Orogen, and the circles the location of corridor 1 sites in the Slave craton. The grey lines show the profiles (boxed 1 and 2) onto which sites were projected for modelling studies. The full name for each site has the prefix "sno", but in this and subsequent figures the sites are labelled using only the last three digits. HR, Hay River terrane; SC, Slave craton. Other tectonic units are as labelled in Fig. 1.

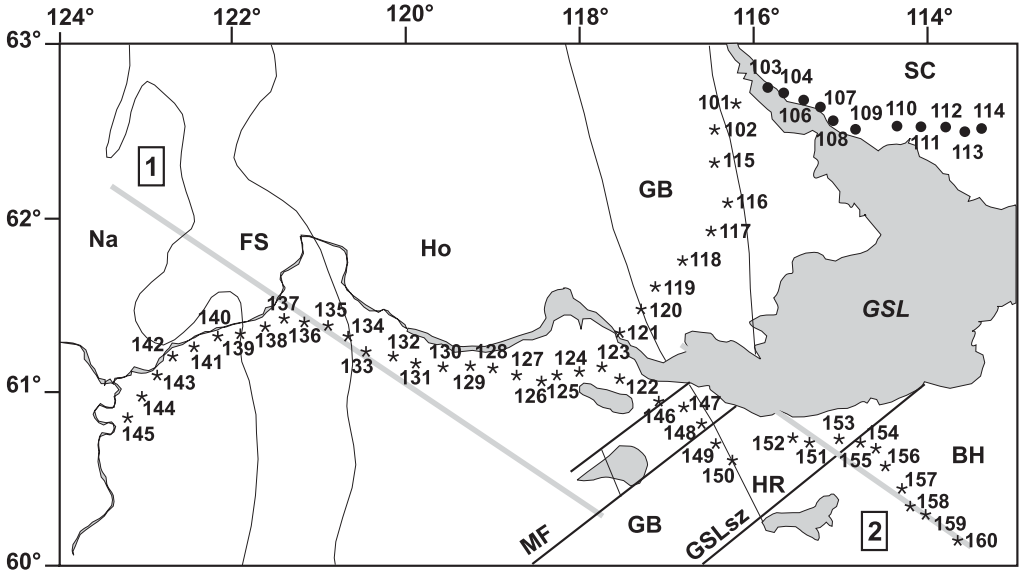

Fig. 3. Example of the eight-decade MT response obtained on the SNORCLE survey. This response is for site 130, which is located in the Hottah terrane. The data are shown for a geographic north–south coordinate system: circles indicate the response corresponding to north–south electric currents (XY mode), and squares the response corresponding to east–west electric currents (YX mode). One standard deviation errors are indicated by vertical bars. For most periods, the bars are smaller than the corresponding symbol.

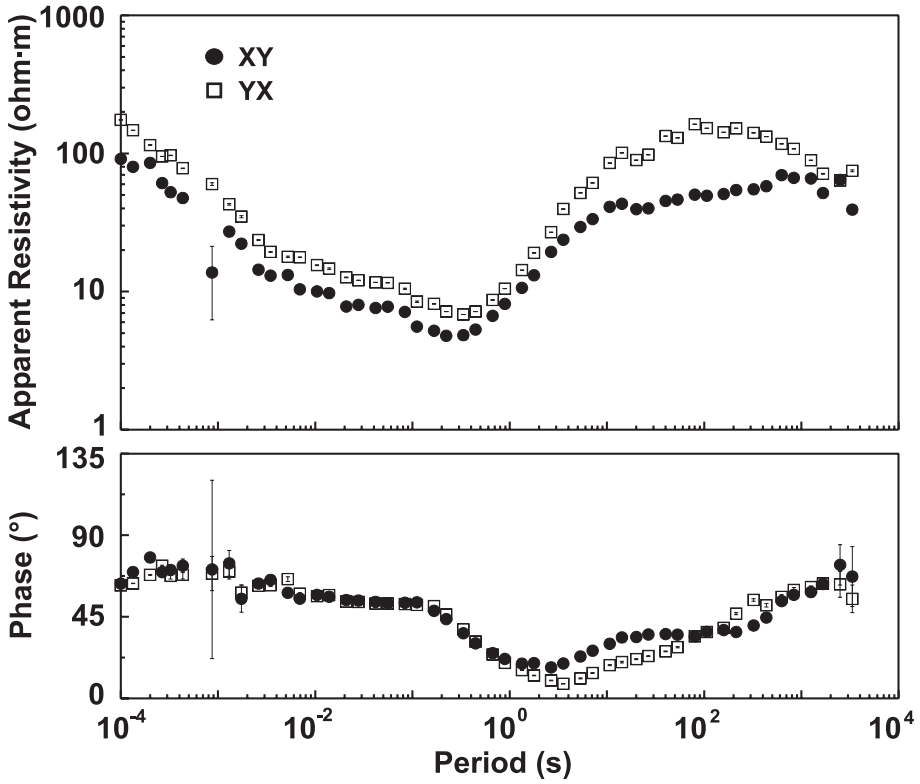

1991; Groom et al. 1993), the geoelectric strike is determined simultaneously with a parameterization of the near-surface galvanic distortion effects.

In the strike-determination methods based on the impedance, there is a 90° ambiguity in the strike orientation. Commonly, the direction of electric current flow for the impedance component with the higher phase response will be the true strike direction, i.e., the TE direction. Thus, if either the

© 2005 NRC Canada

maximum phase split orientation (MPSO) or the GB regional strike azimuths is plotted in the direction of the larger phase term, it will more likely define the true strike. Ambiguity in the strike orientation can also be removed using induction arrows, which are a graphical representation of the transfer function between the vertical and horizontal components of the magnetic field. The direction of the reserved real component of the induction vector will be orthogonal to the local geoelectric strike and for simple 2-D structures will point towards more conductive regions (Parkinson 1962; Jones 1986).

Figure 4 shows strike azimuth results derived from the observed MT response in the Wopmay Orogen and adjacent terranes. At 0.01 s period the maximum phase difference is small at sites located on the Phanerozoic cover (<5°), indicating structures that are close to one-dimensional (1-D) (Fig. 4). Although the phase split is small, the GB regional strike azimuths are closely aligned. The induction arrows have small magnitude, also indicating geoelectric structures that are close to 1-D.

At 10 s period, the GB regional strike and MPSO have an azimuth of N30°E across much of the Wopmay Orogen (Fig. 4). The phase split is typically 15°–25°, indicating moderately strong two-dimensionality. There is a significant change at sites in and adjacent to the Fort Simpson terrane, where small phase differences (<5°) are observed. At 10 s period, the real induction arrows have a magnitude of ~0.2 and a pervasive southward component. This component persists to longer periods and may be caused by the thickening of the Phanerozoic rocks to the southwest of the study area. Alternatively, in contrast to the impedance response, the induction arrows may be significantly affected by the geometry of the source magnetic field. The east–west component of the induction arrow exhibits a significant reversal in the Fort Simpson terrane, indicating the crossing of a conductive zone.

At 100 s period, the GB regional strike directions are rotated 10°–20° clockwise from the azimuth at 10 s period (Fig. 4) and are closely aligned with the MPSO azimuths. The responses cluster in a northeast direction. The phase split at many sites is larger than that at 10 s period and indicates strong two-dimensionality. The reversal of the real induction arrows observed at 10 s period is no longer evident. At 1000 s period, the MPSO and GB regional strike azimuths have predominantly north–south and east–west orientations and the phase splits are significantly smaller than those at at 100 s period.

The penetration depth of electromagnetic signals depends on the local resistivity structure and so for a given period is different in different locations. To more closely relate the observed strike results to geological features, the period of each response was converted to an equivalent depth using the Niblett–Bostick method (Niblett and Sayn-Wittgenstein 1960; Bostick 1977; Jones 1983*a*) and the azimuthally invariant determinant impedance response. Although this depth transform is based on the theory for a 1-D structure, it will provide an approximate depth mapping in more complex structures. Figure 5 shows GB regional strike azimuths for depths centred on 0.5, 5, 15, 25, 70, and 120 km. When interpreting the data it should be noted that the responses represent results averaged over a range of periods or equivalently a range of depths. The lengths of the vectors at each site are scaled so that they are proportional to the difference in phase between the impedance in the two orthogonal directions, providing a measure of the strength of the 2-D structures. Table 1 lists the mean values for the strike direction and phase difference for the different depths.

At 500 m depth, the phase difference at Phanerozoic sites averages 2.5° (Table 1), i.e., the structure is close to 1-D. Larger phase differences observed near the eastern ends of corridors 1 and 1a indicate a contribution to the response from underlying Proterozoic rocks. A rose diagram of the strike azimuths for Proterozoic sites shows that the strikes cluster tightly around an azimuth of N44°E (Fig. 5). Allowing for the 90° uncertainty in the strike determination noted previously, this azimuth may relate to the observed north-northwest–west-northwest strike of the Phanerozoic sedimentary rocks over much of the survey area (e.g., Douglas 1973). Alternatively, it may be an artifact of the tensor decomposition method occurring for nearly 1-D data.

Stronger two-dimensionality is observed at greater depth in the crust in both the Wopmay Orogen and Slave craton. In the Wopmay Orogen the mean phase difference observed at 5 km depth is 7.6° (Table 1). Relatively strong two-dimensionality is observed at sites in corridor 1a near the GSLsz, and very weak two-dimensionality is observed at sites lying on the Fort Simpson basin. The strike directions for the Proterozoic sites are clustered around an azimuth of N32°E (Table 1). The strong east–west component observed in the longer period induction arrows suggests that the azimuth is the true strike. At midcrustal depths of 15 and 25 km, two-dimensionality increases, with the mean phase differences at these periods being 12° and 16°, respectively. The strikes cluster around azimuths of N34°E at 15 km and N36°E at 25 km. Two-dimensionality is particularly strong in the Nahanni terrane and in the western Hottah terrane. It is relatively weak in the Great Bear magmatic arc and extremely weak over the Fort Simpson basin.

At mantle depths in the Wopmay Orogen, two-dimensionality is weaker than that at crustal depths, and at 70 km depth, the mean phase difference is 9° (Table 1). Stronger two-dimensionality occurs only in localized areas. Phase differences of 15°–20° are observed in the Nahanni terrane, in the eastern Hottah terrane, and in the Buffalo Head terrane to the southeast of the GSLsz. The mean azimuth for the responses at 70 km depth is N43°E.

The MT signals are strongly attenuated in conductive regions of the crust and mantle, and at some sites, it is not possible to define an accurate MT response at depths exceeding about 100 km. There is still a sufficient number of accurate responses to define the regional strike azimuth at a depth of 120 km, however. At this depth, allowing for the 90° ambiguity in strike direction, the azimuths for Proterozoic sites form two clusters. Sites in the west of corridor 1 have dominantly east–west or north–south strikes, whereas sites in the east of corridors 1 and 1a have azimuths of N20°W or N70°E; sites in the middle of the Hottah terrane have a transitional character. Assuming the result lies close to north–south, the mean strike for the western sites (sites west of site 126) is N2°W. Examination of the variation of strike angle using smaller period intervals (not presented here) indicates that for the eastern sites the strike azimuth

© 2005 NRC Canada

Fig. 4. Geoelectric strike parameters at 0.01, 10, 100, and 1000 s periods. Abbreviations as in Figs. 1 and 2. (*a*) MPSO azimuth plotted in the direction of maximum phase. The length of the symbol is proportional to the difference between the estimated TE and TM phase, and the scale is shown in the 0.01 s panel. Results are based on the average response for three frequencies centred on the middle of the period band. (*b*) Groom–Bailey (GB) regional strike azimuth. The symbols are plotted in the direction interpreted to correspond to the true regional strike. Results are for one-decade-wide bands centred on the middle of the period band. (*c*) Real induction arrows, plotted with the Parkinson (1962) convention so as to point towards conductive regions. The results are for a single response estimate at the specified period.

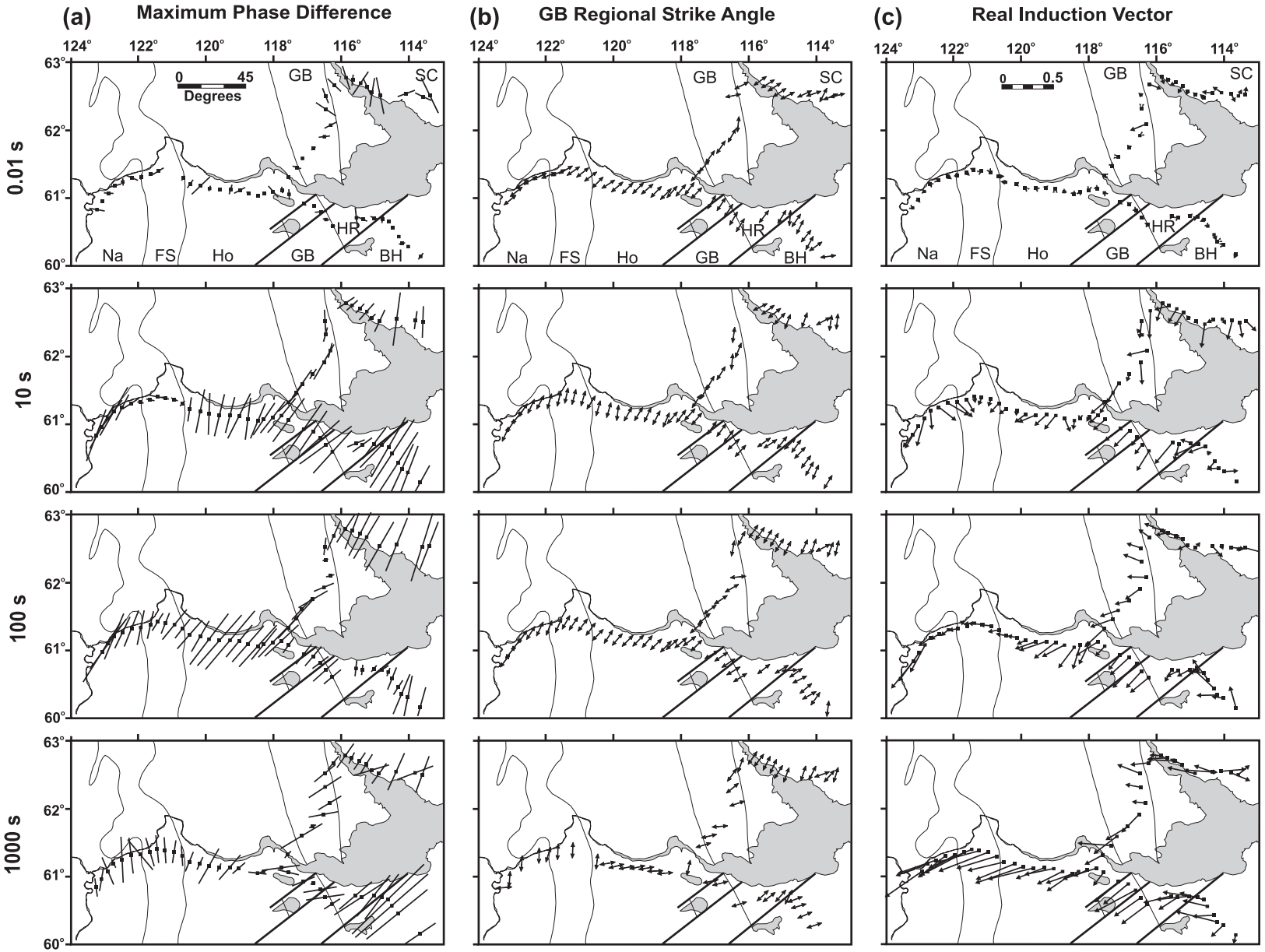

© 2005 NRC Canada

rotates clockwise from its orientation at shallower depths as the period increases. Therefore the true strike azimuth at 120 km depth will lie in the northeast quadrant and will be ~N62°E. The mean phase difference for both sets of strikes is 6° (Table 1).

In summary, the MT response for corridors 1 and 1a suggests the structure is ~1-D at shallow depth at sites located on Phanerozoic sedimentary rocks. It is ~2-D, with a northeast-strike azimuth, at crustal depths. Local variations occur, such as at sites located on the Fort Simpson basin where the response is closer to 1-D. Lastly, at mantle depths the strike direction rotates clockwise. In the uppermost mantle, the strike appears to be centred on ~N42°E and appears to rotate into a more east–west direction with increasing depth.

In this study, the structure of the Phanerozoic sedimentary sequence will be determined using 1-D inversion methods, and the Proterozoic crustal and uppermost mantle structure will be determined using 2-D inversion methods. For the 2-D studies, we adopt a geoelectric strike angle of N34°E, which is the average strike angle for Proterozoic sites for the period range 10^{-1}–10^{3} s. The along-strike (TE) direction is thus N34°E, and the across-strike (TM) direction N56°W. It is possible to include the short-period MT responses (10^{-4}–10^{-2} s) in the 2-D inversions, permitting determination of full crustal sections, because they are so close to 1-D in form. Interpretation of the deeper (>70 km) parts of the resistivity models must include consideration of the effects of the rotation of strike angle at long period.

Apparent resistivity and phase

Figure 6 shows TE and TM apparent resistivity and phase data as contoured pseudosections along corridor 1. The vertical axis corresponds to period increasing downwards, and, as the depth of penetration increases with increasing period, the apparent resistivity image is a smoothed image, or pseudosection, of the true structure. Results are shown in a series of panels to accommodate the changing corridor orientations. For the western part of corridor 1 (left panel in Fig. 6) and corridor 1a, the sites are projected on a line perpendicular to the geoelectric strike and, therefore, represent true 2-D geoelectric sections. Corridor 1 crosses the Great Bear magmatic arc and the western Slave craton at an oblique angle to the geological and geoelectric strike. Therefore, for the eastern part of corridor 1 (middle and upper right panels in Fig. 6), the sites are projected onto straight lines coincident with the survey profile. The TE and TM data remain in the N34°E and N56°W coordinate system, so the resulting sections represent oblique projections of true 2-D geoelectric sections.

The MT response in the Slave craton is distinct from that to the west. Apparent resistivities are much higher and vary more from site to site. The phase response is more spatially uniform, indicating that the apparent resistivity variations are due, at least in part, to galvanic distortion from near-surface structures. As noted by Jones and Ferguson (2001), however, the southwestern part of the Slave craton is highly anomalous for Precambrian terranes in displaying relatively low galvanic distortions.

Farther west in corridor 1, and in corridor 1a, the short-period apparent resistivity response is very conductive, which, based on the penetration depths, can be attributed to the Phanerozoic sedimentary rocks. In the Nahanni terrane, Fort Simpson terrane, Hottah terrane, and western part of the Great Bear magmatic arc, the low apparent resistivity (<50 Ω·m) extends from the shortest periods to periods of about 1 s. This conductive response is observed at progressively shorter periods with distance east in corridor 1 across the Great Bear magmatic arc and can be attributed to the eastward thinning of the Phanerozoic sedimentary rocks.

In the western part of corridor 1, the phase is higher than 45° at periods < ~0.1 s, and < 45° at periods of ~0.1–10 s. The high phase response can be attributed to decrease in resistivity with an increase in depth within the Phanerozoic cover rocks. The low phase response can be attributed to the increase in resistivity at the transition to the underlying crystalline rocks. Note that there is an anomaly in the response near site 136 in which more conductive responses (<10 Ω·m) are observed at short periods. This response is labelled I in Fig. 6 and corresponds to the location of the induction vector reversal (Fig. 4).

The Niblett–Bostick relationship, and alternative period–depth relationships, such as that of Schmucker and Janknowsky (1972), indicates that the period range of 1–10^{3} s corresponds to MT signal penetration from upper crust to upper mantle depths. In this period range, the apparent resistivity values increase along corridor 1 from ~200 Ω·m in the west to ~2000 Ω·m beneath the Great Bear magmatic arc, and to >5000 Ω·m in the Slave craton. Phase increases with increasing period through this period range, with specific phase values being reached at progressively shorter periods with distance to the east. Electromagnetic signal absorption in conductive surface rocks limits resolution of structures in more resistive underlying crust, and the gradual changes occurring in the response from east to west across the corridor can be attributed, at least in part, to the increasing thickness of surface sedimentary rocks.

The observation of localized lateral variations in apparent resistivity and phase at intermediate to long periods along the western part of corridor 1 indicates the presence of strong variations in the resistivity structure of the crust and upper mantle. There is a significant anomaly in the TE response at sites 131 and 130 (labelled I in Fig. 6), in which the TE resistivity is lower (~100 Ω·m) and the TE phase is higher than those at adjacent sites. This anomaly extends from ~1 s to 10^{4} s. In corridor 1a there are significant variations in the TE phase and the TE and TM apparent resistivity response at sites 146–148 (labelled III in Fig. 6). Lastly, there are additional smaller variations in the TE and TM responses within the Fort Simpson and Nahanni terranes.

The signal penetration at 1000 s period is to about 150 km depth in the region of conductive Phanerozoic rocks overlying the Nahanni to Hottah terranes and to more than 400 km in the more resistive conditions of the Slave craton and adjacent Great Bear magmatic arc. At periods > 1000 s, the MT responses in corridors 1 and 1a are characterized by relatively high phase and relatively low apparent resistivity. Lateral variations do occur in this long-period response. For example, in corridor 1 in the eastern part of the Great Bear magmatic arc and in the Slave craton, the decrease in apparent resistivity occurs at longer periods than it does farther to the west in corridor 1 and in corridor 1a. These results sug-

© 2005 NRC Canada

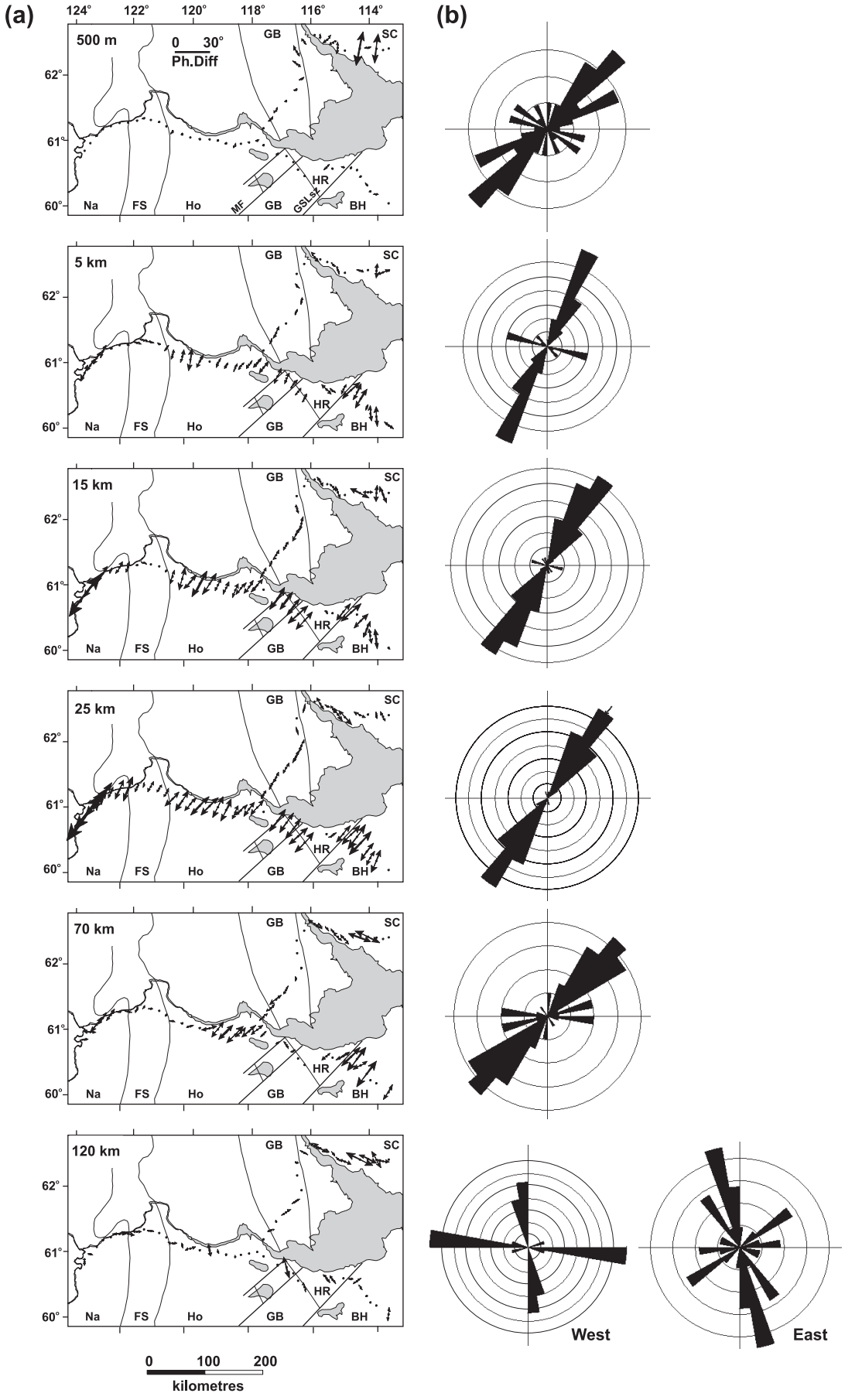

© 2005 NRC Canada

Fig. 5. The GB regional strike orientations along SNORCLE Transect corridors 1 and 1a at depths of 0.5, 5, 15, 25, 70, and 120 km. The GB responses have been converted to approximate depths using the Niblett–Bostick transform. The results for each panel are included for depths within 15% of the central value. The GB azimuths have been plotted in the direction of higher phase, and at some sites the azimuth plotted may be perpendicular rather than parallel to the true geoelectric strike. The length of each symbol is proportional to the difference between the estimated TE and TM phase. (*a*) Strike azimuths shown in map form. Ph.Diff., phase difference. Other abbreviations as in Figs. 1 and 2. (*b*) Synthesis of responses from Proterozoic sites using rose diagrams. Results have been binned into 10° arcs, and the circles correspond to 5% of the total number of responses. The results for 120 km depth have been divided into two overlapping groups of sites: those to the west of site 126 and those to the east of site 129. The number of sites used for each rose diagram is listed in Table 1.

Table 1. Geoelectric strike directions and phase differences for Wopmay Orogen sites.

Depth (km)	No. of sites	Average strike direction	Average phase difference (°)
0.5	42	N44°E	2.5
5	44	N32°E	7.6
15	45	N34°E	12.3
25	46	N36°E	16.0
70	42	N43°E	9.2
120 (west)	15	N1.9°W	5.6
120 (east)	22	N62°W	5.7

gest that the electrical lithosphere is thicker in the northwestern part of the study area.

The smooth apparent resistivity responses observed at sites located on Phanerozoic sedimentary rocks, in the part of the study area outside the Slave craton (Fig. 6), suggest the presence of minimal galvanic distortion due to near-surface heterogeneities. In the GB tensor decomposition method, the phase-related galvanic distortion at each frequency is characterized by shear, which provides a measure of the local polarization of the electric field response, and twist, which provides a measure of its local rotation. The GB shear at sites on the Phanerozoic sedimentary rocks is typically < 10° at periods < 300 s (cf. a value of 45° for complete polarization of the electric field), confirming the low levels of distortion (Wu 2001). The shear at periods exceeding 300 s reaches values of 10°–25°, suggesting the presence of heterogeneity in the Proterozoic crust. Analyses of the apparent resistivity responses using the methods of Sternberg (Sternberg et al. 1985) and Jones (1988) indicate the level of static shift at the MT sites is typically < 10% (Wu 2001).

Geoelectric structure

Phanerozoic sedimentary rocks

The MT apparent resistivity and phase responses show that the Phanerozoic sedimentary rocks form a relatively thick, conductive, surface layer along the western parts of corridors 1 and 1a. The internal structure of these rocks is investigated using 1-D inversion techniques in which the observed data at each site are fitted by horizontally layered resistivity models. The inversions were based on the determinant impedance response at periods of <10 s and used the Fischer et al. (1981) 1-D inversion method, in which the data were fitted by a model containing as many layers as can be justified statistically by the data fit. Figure 7 shows an image of the 1-D models, stitched together, for the different sites along corridors 1 and 1a.

There is good consistency between the models for different sites, allowing the resistivity structure to be divided into several zones. There is a moderately resistive upper layer (>50 Ω·m) resolved along much of the profile. This layer is observed most consistently in eastern Fort Simpson and western Hottah terranes, where it is 20–100 m thick. Along most of corridor 1 and the western part of corridor 1a, the resistive surface zone is underlain by a very conductive layer (~10 Ω·m). The thickness of this layer decreases from 1000 m at site 139 in the Fort Simpson terrane to 200 m at site 118 in the Great Bear magmatic arc. The conductive layer also thins abruptly to around 200 m at sites 142 and 143 over the Bulmer Lake High. The anomaly I on the response pseudosection in Fig. 6 is associated with a local decrease in the resistivity of the near-surface rocks in this area. In the eastern part of the Great Bear magmatic arc in corridor 1 (sites 101–117), the near-surface rocks are more resistive (~100 Ω·m). In corridor 1a, there is a significant change in the near-surface structure at sites 151 and 152. This change occurs at the Presqu'ile barrier. To the east of this point, the near-surface rocks form two layers, with a 300–400 m-thick layer of 500 Ω·m overlying a 200–300 m-thick layer of 20 Ω·m.

Wu (2001) completed a more detailed interpretation of the resistivity structure of the Phanerozoic rocks and compared the MT results with resistivity logs from oil industry wells along the corridors. After correction of minor static shift effects in the MT data, the integrated conductance of the upper layers of 1-D resistivity models is in good agreement with that of sedimentary rocks determined from induction logs. Similarly, the depth to the resistive basement derived from the MT models is in good agreement with that indicated by the resistivity logs. Much of the observed 1%–10% misfit in conductance and depth can be attributed to subsurface variations over the ~10 km distance between each borehole and the nearest MT site.

Proterozoic crust and lithosphere

The 2-D structure of the crust and upper mantle was determined for profiles, drawn in Fig. 2, including the western part of corridor 1 and corridor 1a. Because corridor 1 crosses the Great Bear magmatic arc at a small angle to the geological and geoelectric strike, the sites from this part of the corridor could not be modelled using 2-D methods. The inversion methods used were the 2-D Occam inversion method of deGroot-Hedlin and Constable (1990) and the nonlinear conjugate gradient (NLCG) method of Rodi and Mackie (2001). The 2-D Occam inversion, which is based on

© 2005 NRC Canada

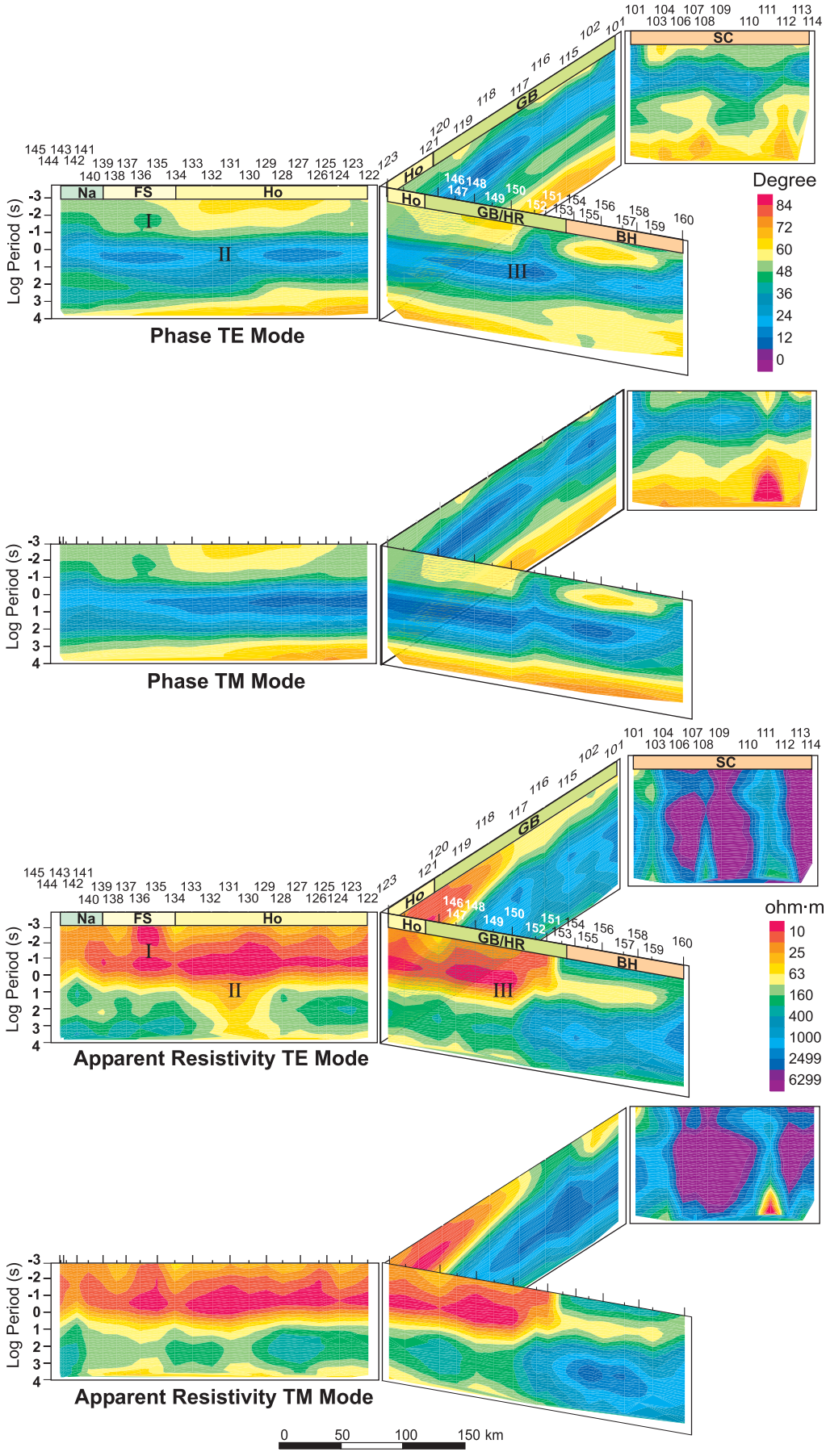

© 2005 NRC Canada

Fig. 6. Apparent resistivity and phase pseudosections for TE and TM modes along corridors 1 and 1a. The results are presented as a fence plot, with the individual panels coinciding with the locations of the sites. Tectonic elements crossed by the sections are indicated by lettering at the top using the same abbreviations as in Figs. 1 and 2. Responses for the western portion of corridor 1 and for corridor 1a have been projected onto a line orthogonal to the geoelectric strike of N34°E prior to plotting and represent true 2-D sections. Responses for the Great Bear and Slave portions of the corridor have been projected onto lines parallel to the acquisition corridor and are therefore oblique geoelectric sections. Features labelled I–III are discussed in the text.

Fig. 7. One-dimensional resistivity models for corridors 1 and 1a stitched to form a continuous section.

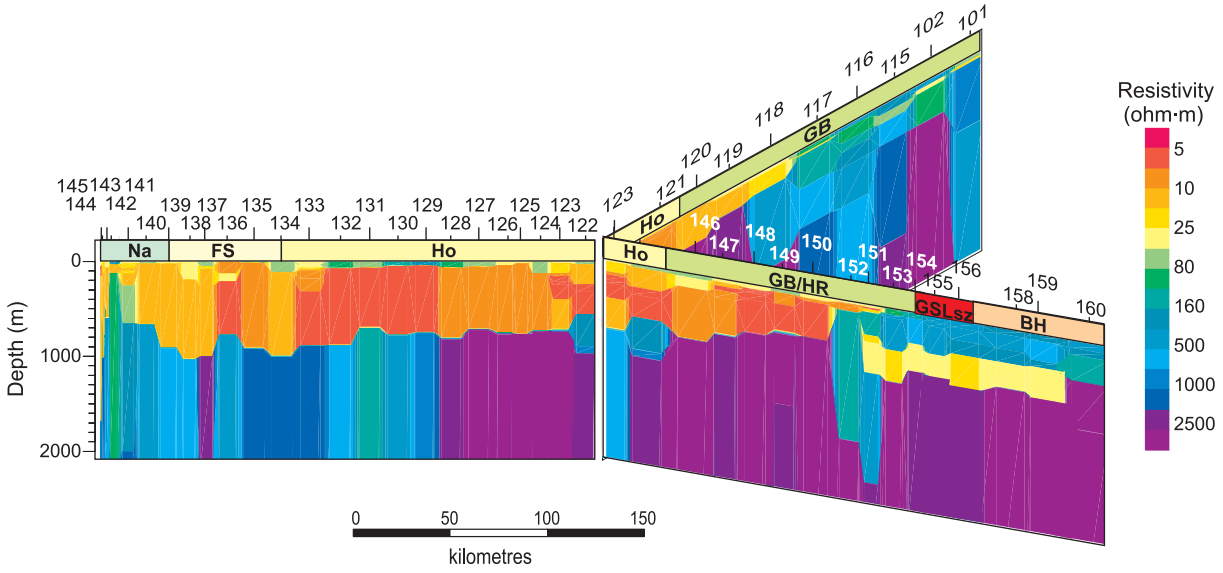

the forward modelling code of Wannamaker et al. (1987), determines the model with minimum roughness that fits the data to a specified level of misfit. The NLCG algorithm, which is based on a finite-difference forward modelling code, minimizes an objective function incorporating the misfit between the model response and observed data and the roughness of the model.

More than 30 two-dimensional inversions have been done to determine the resistivity structure and investigate the resolution of features in the resistivity models. Inversions have been done for the following data and inversion parameters: (*i*) different subsets of the data, i.e., TE data (with and without induction arrows), TM data, and joint TE + TM data; (*ii*) data corrected for galvanic distortion using the GB method and uncorrected data; (*iii*) starting models consisting of uniform half-spaces of different resistivity and consisting of the shallow resistivity structure determined from the 1-D inversions superimposed onto a uniform half-space; (*iv*) different values of the smoothing parameter τ, which controls the trade-off between minimizing the data misfit and minimizing the model roughness, in the NLCG inversions; (*v*) different error floors on the apparent resistivity and phase data; and (*vi*) data projected into several different coordinate systems, with the strike direction ranging from N34°E to N62°E.

The majority of the inversions were done using separate, overlapping, profile segments corresponding to corridors 1 and 1a. This approach was adopted because the corridor 1a data were included in the study later than the corridor 1 data and because of limitations to the size of the models that could be considered in the 2-D Occam inversions. Inversions have since been done using data for the whole profile to ensure that features in the resistivity models near the intersection of corridors 1 and 1a are not spurious edge effects.

The resistivity models shown and interpreted herein are those corresponding to NLCG and Occam inversions of combined TE (excluding induction arrows) and TM datasets. The data that were inverted were rotated to the regional strike angle of N34°E and corrected for minor shear and twist components of galvanic distortion determined in the GB analysis. They were not corrected for static shift. Error floors were applied in the inversion, with larger errors applied to the apparent resistivity response to allow for the effects of static shift. The phase error floor was equivalent to a 5% error on the MT impedance, and the apparent resistivity error floor was equivalent to 10% error on the impedance.

The normalized root mean square (RMS) misfits of the final TE + TM inversion models are 1.69 (Occam) and 1.65 (NLCG) for the western segment and 2.84 (Occam) and 2.09 (NLCG) for the eastern segment. Figure 8 shows the fit of the NLCG inversion-model responses to the observed responses at eight representative sites along corridors 1 and 1a, and Fig. 9 compares the phase responses for the NLCG model, the Occam model, and the observed data. The data fit is generally good, with the TM model responses fitting the data better than the TE responses, and the fit at short periods (<10 s) being better than that at long periods. The misfit at periods longer than several hundred seconds may be due in part to a three-dimensional (3-D) response caused by the rotation of geoelectric strike shown in Figs. 4 and 5. The poorer fit of the TE response is consistent with this interpretation (Swift 1967; Jones 1983*b*; Wannamaker et al. 1984). Comparison of the observed and model responses (Figs. 8

© 2005 NRC Canada

Fig. 8. Comparison of the response of the TE + TM NLCG inversion model and the observed response for every fourth site along corridor 1 and the western part of corridor 1a. The results shown are typical of those at adjacent sites. Results for the eastern part of corridor 1a are shown in Wu et al. (2002).

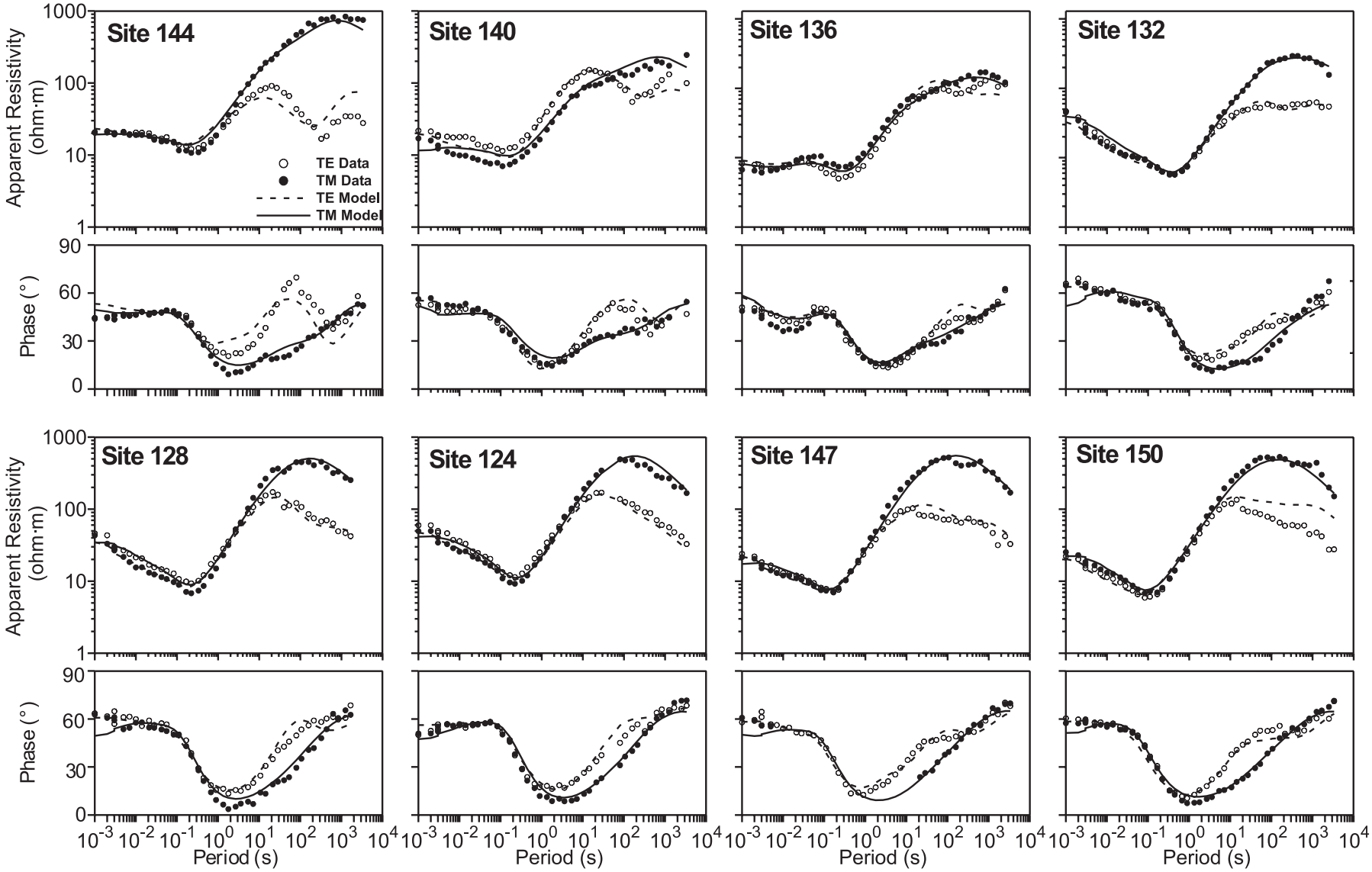

© 2005 NRC Canada

Fig. 9. Comparison of the observed and model phase responses. Every fourth site on each profile is labelled. (*a*) Observed TE and TM GB phase response. (*b*) Phase response of the 2-D NLCG model. (*c*) Phase response of the 2-D Occam model.

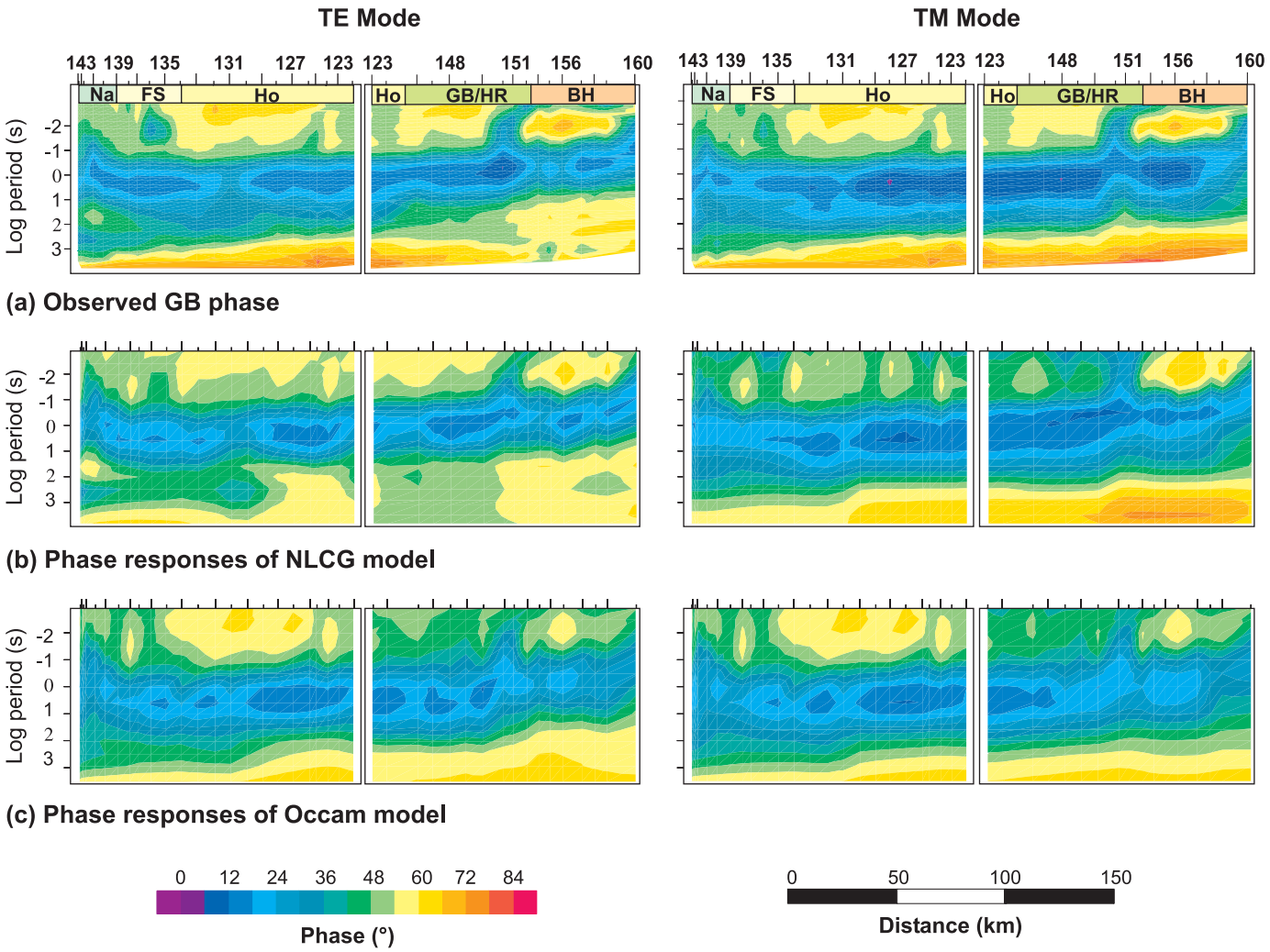

and 9) indicates that the NLCG model provides a superior fit to the data at intermediate periods (0.1–100 s), whereas the Occam model provides a superior fit at both short periods (<0.1 s) and long periods (>100 s).

Figure 10 shows the final 2-D Occam and NLCG inversion models. The similarity of the major geoelectric structures obtained using the two different inversion methods provides confidence that these structures are required features of the data, rather than artefacts introduced by the inversion algorithms. There are some minor differences between the models, e.g., in the upper mantle at the edge of the western panel. The models were all discretized as finely as allowed by the computers and software used in the inversions. With these limitations, the NLCG model was discretized more finely than the Occam model and is considered the overall superior model. The better fit of the Occam model at short and long periods suggests, however, that this model may be superior for the Phanerozoic sedimentary rocks and for the lithospheric mantle.

Specific structures in the 2-D resistivity models are now examined in more detail. In particular, we use the results from multiple inversions to examine the resolution of the different structures and to assess to what extent they are necessary features of the true resistivity structure.

(1) The 2-D models include shallow conductive structures similar to those resolved in the 1-D modelling. At depths of less than a few kilometres, the 1-D inversion models were parameterized more finely than the 2-D models and therefore provide better resolution of the vertical variations in the near-surface resistivity structure. In contrast, the 2-D inversions include horizontal smoothing, so the 2-D inversion models probably provide a superior representation of the lateral variations in the near-surface resistivity. The overall agreement of the 1-D and 2-D results shows that the 1-D approach is valid and, in particular, that the large-scale variation in the thickness of the Phanerozoic rocks causes no biasing of the local MT response.

The induction-arrow reversal at 10 s period (Fig. 4) is most likely caused by resistivity variation within the Phanerozoic sedimentary rocks. As noted previously, the reversal, which occurs at sites sno135 and sno136, is coincident with decreased apparent resistivity at periods of 10^{-3}–10^{-1} s (feature I in Fig. 6). The shallow part of the

© 2005 NRC Canada

Fig. 10. Two-dimensional resistivity models for the western portion of corridor 1 and for corridor 1A. The results are based on inversion of the TE and TM MT responses. Labelled structures A–I are discussed in the text. Abbreviations as in Fig. 1. (*a*) Shallow part of Occam model shown at ~10 times vertical exaggeration. (*b*) Two-dimensional NLCG inversion model. (*c*) Full 2-D Occam inversion model. Similarity of structures in the Occam and NLCG models provides an indication of resolution.

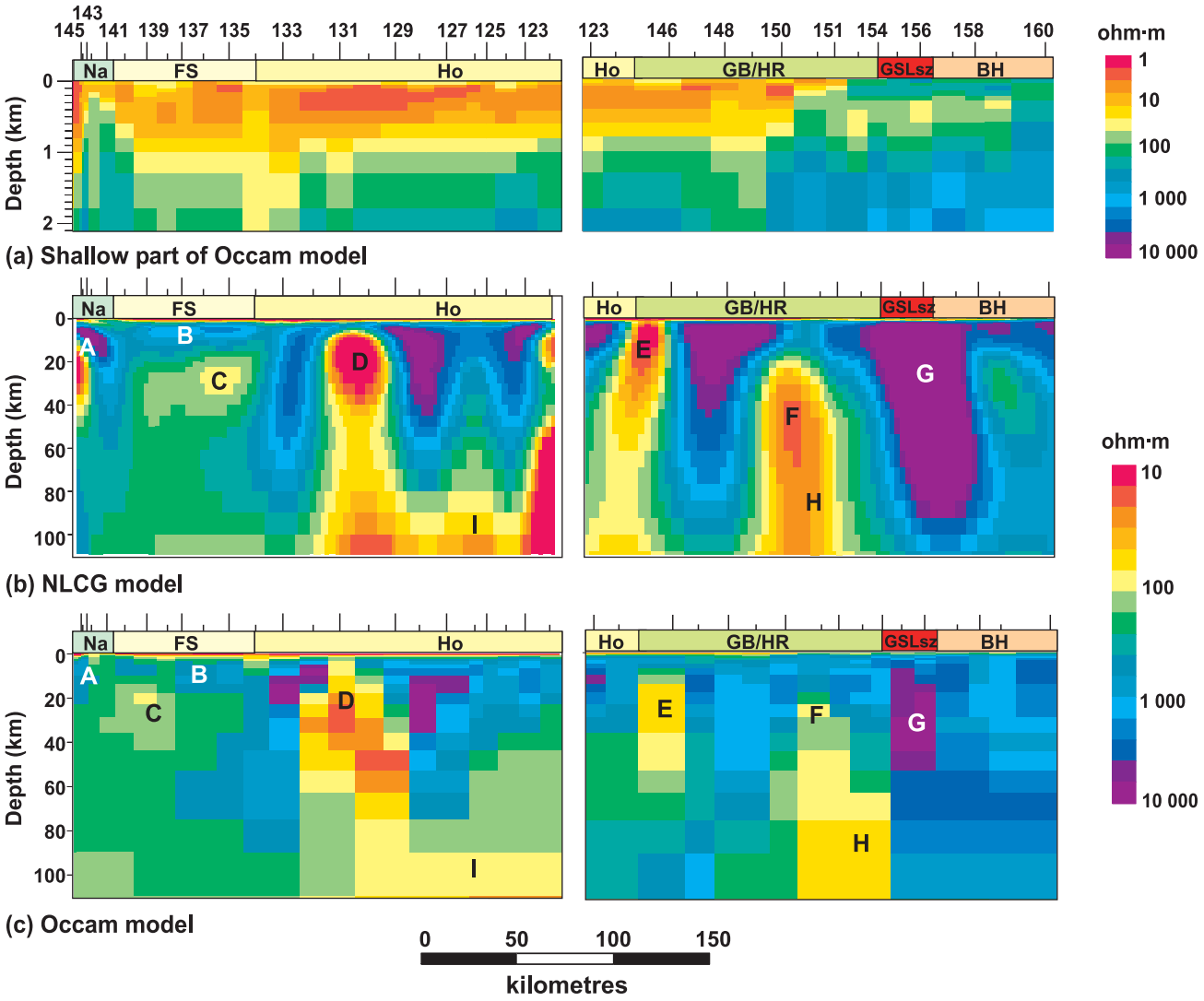

2-D resistivity models requires relatively low resistivity near sites sno135 and sno136 (Fig. 10*a*) to fit this apparent resistivity feature.

It is initially surprising that a near-surface structure affecting the apparent resistivity at periods as short as 10^{-2} s should have a significant effect on induction arrows at periods as long as 10 s, but 2-D forward modelling confirms this result. MT and induction arrow responses were computed for a range of 2-D models that included locally decreased resistivity within a near-surface layer with thickness and resistivity similar to those along corridor 1. For all of the models considered, the locally decreased resistivity affects the apparent resistivity response at periods between 10^{-3} and 1 s and causes an induction-arrow reversal, with the largest response at a period of about 10 s. These results mean that the observed induction-arrow reversal along corridor 1 can be attributed to variations within the near-surface sedimentary rocks with a reasonable degree of confidence.

The final inversion models presented here did not include induction arrows in the dataset. A number of Occam inversions included both the induction-arrow and MT data, with a range of different error floors for this data, but none provided a simultaneous fit to both datasets. This may be because computer memory limitations prevented the use of enough frequencies to adequately define both the short-period effect of near-surface structure in the MT response and its longer period effect in the induction-arrow response.

(2) A relatively resistive body is present in the upper crust in the western Fort Simpson terrane, labelled B in Fig. 10. This body is resolved more clearly in the NLCG model, where it has a resistivity >1000 Ω·m, than in the Occam model. The depth to the bottom of the body increases from about 10 km under site sno133 to about 20 km under site sno138 and is approximately constant farther to the east between sites sno138 and sno140. At sites above this body the 10 s phase differences are much smaller

© 2005 NRC Canada

than those at surrounding sites (Fig. 4). The body is underlain by a relatively conductive zone (~130–250 Ω·m), labelled C in Fig. 10. The MT method provides reasonable resolution of the depth to conductive bodies, so the interface between the resistive region in the upper crust and the underlying conductive zone will be quite well resolved.

(3) A prominent conductive zone (<30 Ω·m) is present beneath sites sno131 and sno130 (labelled D in Fig. 10). The top of the zone is at around 10 km depth. There is strong support for the existence of this body in both the NLCG and Occam models and in the geoelectric response, which exhibits low apparent resistivity and high phase in the TE component at this location (labelled II in Fig. 6). Because of the low resistivity of the body, the depth to its base is not well resolved. Resolution of the true geometry of the body is also restricted because of the conductive near-surface sedimentary rocks.

(4) The lower crust beneath the Great Bear magmatic arc and Hay River terrane contains two conductive zones (<60 Ω·m) (labelled E and F in Fig. 10) separated by a more resistive zone beneath sites sno148 and sno149. These features are associated with significant lateral changes in the TE and TM mode responses at periods >1 s. The western zone of low resistivity (feature E in Fig. 10) occurs near the intersection of the two inversion models and has lower resistivity in the NLCG model than in the Occam model. These observations made it important to assess whether the structure may be a spurious feature appearing at the edge effect of the inversion models. Resistivity models derived from NLCG inversions of a combined corridor 1 and corridor 1a dataset include a zone of low resistivity similar to that in Fig. 10*b*, confirming that it is a structure required by the data.

(5) There is a near-vertical resistive zone beneath the surface location of the GSLsz (labelled G in Fig. 10). At mantle depths this crustal feature is underlain by an abrupt transition between a more conductive zone to the west and a more resistive zone to the east (labelled H in Fig. 10). The response of the GSLsz is modelled in more detail and discussed in Wu et al. (2002) and is not considered further in the present study.

(6) There is a broad zone of low resistivity (<150 Ω·m) at >60 km depth in the mantle beneath the Hottah terrane and Great Bear magmatic arc (labelled I in Fig. 10). This structure is required to fit decreased apparent resistivity and increased phase in the long-period TE response. It also appears in inversions of combined corridor 1 and corridor 1a datasets and in inversions done using more east–west strike angles. These results indicate that the structure is a required feature of the MT data and that it is not an artefact of the change in strike angle at long periods.
The zone of low mantle resistivity is located 200 km north of the Kiskatinaw Conductor in northern Alberta (Boerner et al. 2000). Because of this distance it is unlikely that the decreased resistivity in feature I, which occurs as shallow as 60 km depth, is caused by large-scale 3-D effects associated with the Kiskatinaw Conductor. The absence of an enhanced southwards component in the long-period induction-arrow response above feature I (Fig. 4) supports this interpretation.

(7) The Occam and NLCG models resolve different structures in the crust at the margin of the Nahanni and Fort Simpson terranes in the area labelled A in Fig. 10. Detailed modelling of the data from this area shows that such structures are required at crustal depth in the resistivity models to fit a divergence between the observed TE and TM mode responses at long periods which is particularly strong at sites to the west of sno141. Although the MT data indicate the presence of 2-D structure, because of the low resistivity of the crust and the low resistivity of the overlying Phanerozoic rocks, the method is unable to constrain the specific structures that are present.

Interpretation of Precambrian resistivity structures

Crustal strike directions in the Wopmay Orogen

At crustal depths the geoelectric strike at most MT sites in the Wopmay Orogen is N30°E–N40°E. This azimuth is oblique to the interpreted terrane boundaries within the Wopmay Orogen (and to the potential-field anomalies upon which these boundaries are defined) and cannot be explained in terms of resistivity structures aligned with the boundaries.

In the exposed rocks of the Wopmay Orogen to the north of the study area the most prominent structural feature is regional-scale transcurrent faulting that creates a pervasive northeast to southwest geological fabric (Hildebrand et al. 1987; Hoffman 1989). This faulting occurred post-1.84 Ga and pre-1.66 Ga in response to either the Fort Simpson – Hottah collision (Hildebrand et al. 1987) or the docking of a Nahanni terrane (Hoffman 1989). It consists of a conjugate set of dextral northeast-trending faults and sinistral northwest-trending faults that resulted in irrotational east–west shortening and north–south extension that regionally exceed 20% (Hoffman 1989). Within the Great Bear magmatic arc most of the faults are steeply dipping to vertical, with up to several kilometres of strike-slip displacement (Hildebrand et al. 1987). Considering the scale of the transcurrent faulting and the tectonic events to which it is attributed, it is probable that the faulting extends well southward beneath the Phanerozoic cover.

The geoelectric strike in the crust is subparallel to the transcurrent faulting (Fig. 11). The geoelectric strikes are centred on a slightly more north–south azimuth than the faulting, but this difference may be explained by a rotation of the fault azimuths at latitudes near the southern limit of the Slave craton. The MT and surface geological observations thus provide a strong indication that the geoelectric response is related to the faulting. In this case, the observed geoelectric strike may be explained by the juxtaposition of crustal blocks of differing resistivity across northeast–southwest-striking boundaries formed by the faults. Conductive zones formed at terrane margins prior to the faulting would also be extended in the northeast–southwest direction, contributing to the observed strike.

The same geoelectric strike azimuth is observed in the Nahanni terrane as in the Hottah terrane and Great Bear magmatic arc, providing a strong indication that the same

© 2005 NRC Canada

Fig. 11. Comparison of observed MT strike azimuth at 15 km depth with major faults. Geology is from Wheeler et al. (1997). The strike azimuths at MT sites in the Wopmay Orogen are subparallel to faults mapped in the exposed Wopmay Orogen to the north of the Lithoprobe transect. The exposed Wopmay Orogen is labelled Wop and shaded white; faults are shown as grey lines.

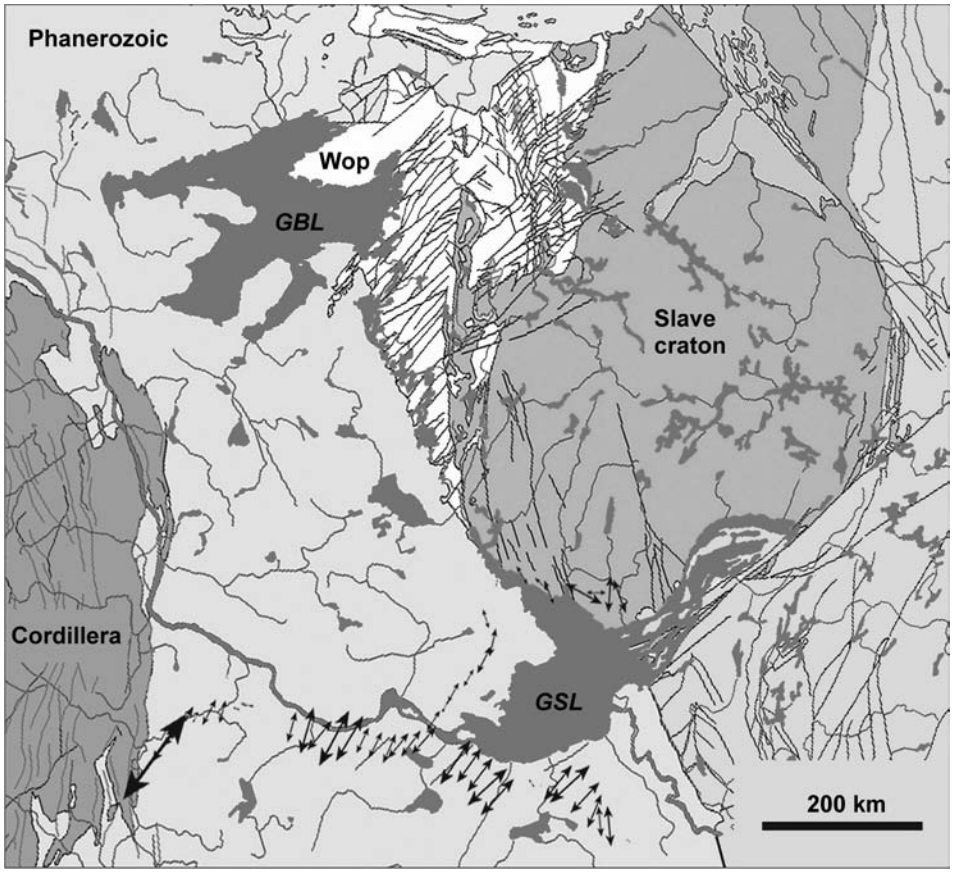

Fig. 12. Models of terrane accretion in the Wopmay Orogen accounting for the observed geoelectric strike at crustal and mantle depths. The models must explain the relatively uniform crustal strike azimuth across the orogen, including the Nahanni terrane, and subparallel crustal and mantle strike azimuths. Abbreviations as in Fig. 1. (*a*) Nahanni terranes collide with Hottah terrane, causing transcurrent faulting and creating the geoelectric fabric across the orogen. Partial crust–mantle coupling is required to explain the mantle azimuth. (*b*) Same as the previous model except the faulting is caused by the collision of already docked Nahanni and Fort Simpson terranes. (*c*) Oblique collision of western terranes causing subparallel deformation at crustal and mantle depths. The Fort Simpson basin formed after events in (*a*)–(*c*) resulting in a weaker 2-D response and a more north–south strike azimuth at sites overlying the basin.

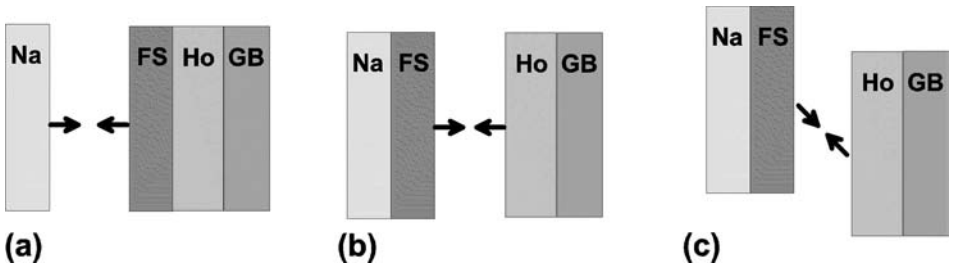

events are responsible for the structures in both terranes. The results are consistent with the interpretation that it was the docking of the Nahanni terrane that caused the transcurrent faulting (Fig. 12*a*). Alternatively, if the observed strikes are related to the terminal collision of both the Fort Simpson and Hottah terranes, the results indicate that the Nahanni terrane was either docked to the Fort Simpson terrane prior to the collision or in fact represents part of the same terrane (Fig. 12*b*).

Phase differences in the Fort Simpson terrane are very small, indicating structures are close to 1-D. Due to this one-dimensionality, strike azimuths are poorly resolved at these sites but are generally more north–south than in surrounding areas. These responses are interpreted to be associated with the thick sequence of Proterozoic sedimentary rocks in the Fort Simpson basin. The change in strike angle over the basin is consistent with the interpretation that these rocks were deposited after the regional transcurrent faulting occurred.

© 2005 NRC Canada

Mantle strike directions in the Wopmay Orogen

Strike directions observed at uppermost mantle depths in the Wopmay Orogen show a remarkable correlation with those at crustal depths. Northeast strikes, oblique to terrane boundaries, are observed across the whole Wopmay Orogen. Two-dimensionality is strongest in localized areas, but the rose diagram results show a clear clustering of the data from the sites. The centre of the cluster, at N43°E azimuth, is rotated slightly clockwise from the corresponding azimuth (~N34°E) at crustal depths. The similarity of the strike angles at crustal and mantle depths, extending over a region from the Slave craton to the Nahanni terrane, provides a strong indication that the same tectonic event was responsible for producing both sets of structures. We hypothesize that the geoelectric strike at periods corresponding to mantle penetration results from the same event that produced the upper crustal strikes, the docking of the Nahanni terrane, or an amalgamated Nahanni – Fort Simpson terrane to the Wopmay Orogen.

Although the deformation at crustal and mantle depths is interpreted to be due to the same collisional event, on rheological grounds its manifestation would be expected to have had quite a different form. As noted previously, the upper crustal deformation is interpreted to be brittle transcurrent faulting accommodating in excess of 20% east–west shortening. Deformation of the mantle lithosphere in response to these collisions is likely to have been of a more ductile form, since the shallow mantle lithosphere would have had relatively high temperatures following magmatism associated with the eastward and westward subduction that occurred prior to the closing of the Coronation margin and the eastward subduction prior to Fort Simpson collision.

A simple ductile accommodation of east–west shortening and north–south extension would be expected to produce north–south flow and a geoelectric strike with a north–south orientation. The observation of a northeast geoelectric strike in the mantle therefore suggests the existence of kinematic coupling between the upper crust and the mantle lithosphere. Such coupling is proposed to have linked the dominantly northeast dextral motion in the crust to northeast-directed ductile shearing in the mantle (Fig. 12).

The collision of the Fort Simpson terrane was accommodated at midcrustal levels by the delamination of Fort Simpson crust above and below the wedge of Hottah crust. This accommodation would be expected to reduce the coupling between the upper crust and the mantle lithosphere. The results provide support for the interpretation that it was the docking of a separate Nahanni terrane (Fig. 12*a*) rather than the Fort Simpson terrane (or a composite Fort Simpson – Nahanni terrane, Fig. 12*b*) that caused the deformation recorded by the geoelectric strikes. The form of the structures developed at midcrustal levels between the Nahanni and Fort Simpson terranes is unclear; the MT coverage available in this area is limited and the crustal structures have been obscured by the younger extension in that area.

An alternative explanation for the similarity of the crustal and mantle strikes is that both the mantle and crustal deformation were caused by an oblique collision between the Nahanni terrane (or a combined Nahanni – Fort Simpson unit) and the Wopmay Orogen (Fig. 12*c*). In this case the northeast-striking structures could have developed independently at crustal and mantle depths without the requirement of coupling between them. This interpretation is not supported by the accepted interpretations of the exposed structures in the northern Wopmay Orogen (e.g., Hildebrand et al. 1987).

The deepest geoelectric strikes determined from the MT data have different azimuths in the east and west of the Wopmay Orogen. In the east, the strike rotates farther clockwise from its value at shallow depth in the mantle to a value of N62°E at ~100 km depth. This azimuth may be attributed to either the same deformational processes causing the strike at more shallow depths in the mantle lithosphere, or to shearing at the base of the lithosphere associated with modern plate motion, hypotheses discussed in more detail later in the paper. In the west of the survey area, the strike direction is either north–south or east–west and is orthogonal to the trend of the Fort Simpson basin. The strikes are interpreted to be associated with the extension that produced the overlying Fort Simpson basin.

Resistivity structure of the Fort Simpson basin

The MT modelling reveals a relatively resistive (>400 Ω·m) west-dipping body in the Fort Simpson terrane extending to a maximum depth at its western edge of around 20 km (feature B in Fig. 10). The depth to the base of this body will be quite well resolved by the MT method, which provides good resolution of the depth of resistivity decreases and thus the depth of the underlying layer. The geometry of this body correlates closely with seismic reflection data that show a package of westward-dipping (20°–30°) reflections beneath stations 0–2500 (Cook et al. 1998), corresponding to the location of MT sites sno142–sno132. The base of both the reflection package and resistive rocks is at around 20 km (Fig. 13). Seismic refraction data reveal a relatively low velocity in this area (Fernández Viejo et al. 1999; Fernández Viejo and Clowes 2003).

The seismic reflection package has been interpreted to correspond to the Fort Simpson basin, which overlies the Fort Simpson terrane (Cook et al. 1998). The MT results provide confirmation of the geometry of the basin interpreted from the seismic data (Fig. 13). The resistivity models do not provide discrimination between the three zones in the basin defined on the basis of the reflectivity (Cook et al. 1999), but they do show that the Proterozoic rocks deposited in the basin are relatively resistive and significantly more resistive than the underlying crust. The base of the resistive zone correlates quite well with seismic reflections FS1 and FS2. FS1 is interpreted by Cook et al. (1999) to be a thrust, and FS2 defines the base of the monocline extending to the west.

The observed resistivity of the Fort Simpson basin rocks is consistent with that observed in other deposits of undeformed Proterozoic clastic sedimentary rocks. For example, Gupta and Jones (1990) determined a resistivity of 1500 Ω·m for the Proterozoic sedimentary rocks, alluvial-fan and megabreccia-landslide deposits, in the Lewis thrust sheet of southeastern British Columbia. The resistivity may be somewhat enhanced by intrusive igneous rocks. Euler deconvolution modelling of magnetic anomalies indicates the presence of magnetic sources within the Proterozoic sedimentary rocks, and Aspler et al. (2003) speculate these may arise from sills, flows, or dykes.

© 2005 NRC Canada

Fig. 13. Comparison of MT and seismic data along Lithoprobe corridor 1 in the western part of the Wopmay Orogen. Interpreted crustal and mantle units are labelled in blue italic with the following abbreviations. FSB, Fort Simpson basin; FSC, Fort Simpson crust; HC, Hottah crust; PHC, post-Hottah crust; HM, Hottah mantle; FSM, Fort Simpson mantle. (a) Overlay of seismic reflection results and resistivity models based on a seismic velocity of 6 km/s. Seismic reflection data are from Clowes (1997), and their interpretation is from Cook et al. (1998, 1999). FS1, FS2, JH, TW, Su1, Su2, HC4, and HC5 are major seismic reflections or packages of uniform reflectivity defined by Cook et al. (1999) and discussed in the text. (b) Seismic refraction results for corridor 1 (after Fernández-Viejo and Clowes 2003). Thick black lines denote significant wide-angle reflections. Reflection J is defined by Fernández-Viejo and Clowes (2003) and is discussed in the text. M, Moho reflection.

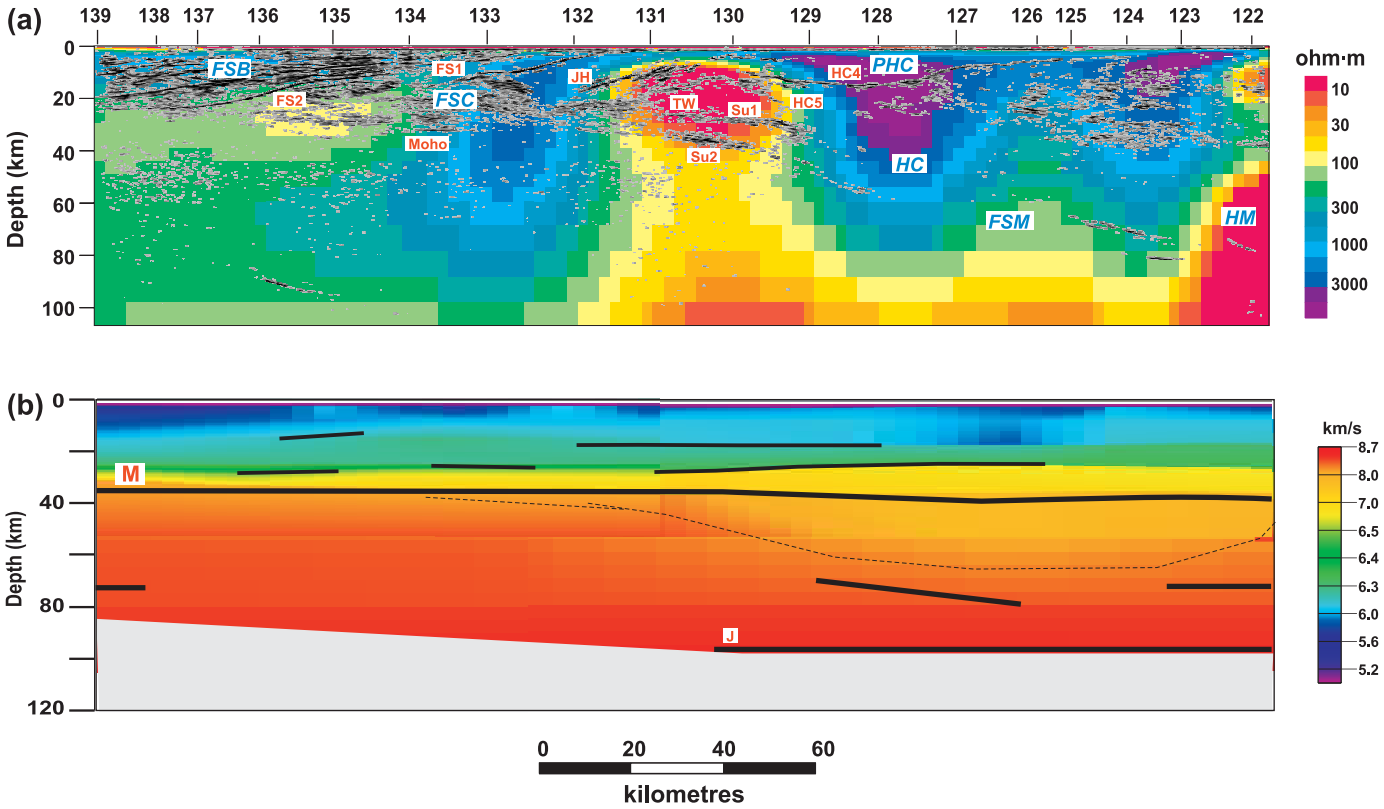

The geoelectric strike observed at sites located on the Fort Simpson terrane differs from that in surrounding areas. At upper crustal depths, the zone of anomalous strike responses is approximately 60 km wide. The two-dimensionality is weak in this zone and the geoelectric strike is parallel to the interpreted trend of the Fort Simpson basin. These responses are interpreted to be due to structures created during formation of the basin.

The MT models reveal that the crust beneath the Fort Simpson basin is more conductive than surrounding areas (zone labelled C in Fig. 10). This result can be established by 1-D modelling and 2-D Occam and NLCG inversions and is therefore considered quite reliable. The differences between the NLCG and Occam models demonstrate, however, that specific features in this part of the crust cannot be resolved. Seismic reflection results reveal structures, postdating deposition of part of the Proterozoic sedimentary sequence, extending into the lower crust (Cook et al. 1999), which suggests that the decreased resistivity may be due to modification of the Precambrian basement.

It is of note that a zone of anomalous MT strikes is observed beneath the Fort Simpson basin at mantle depth, suggesting the lithosphere preserves evidence of the processes occurring during the formation of the basin or rifting. The width of the anomalous zone in the crust is around 100–150 km, but the zone becomes much broader in the mantle, extending to near the middle of the Hottah terrane (Fig. 5).

Fort Simpson – Hottah conductor

The MT models reveal a prominent conductive zone (<100 Ω·m) in the crust beneath sites sno132 to sno130 (labelled D in Fig. 10). Comparison of the NLCG and Occam models suggests that the top of the conductor lies between 5 and 10 km depth and that the conductor extends to significant depth in the crust. The MT models have sufficient resolution to localize this conductive zone at the margin of the Fort Simpson and Hottah terranes, and the conductor is interpreted to be associated with the collision between these terranes.

Comparison of the seismic reflection data and resistivity models (Fig. 13) suggests that the decreased resistivity occurs within the westward-extending midcrustal wedge of Hottah crust interpreted by Cook et al. (1999) and Snyder (2000). The conductor appears to lie in a region between west-dipping reflection JH (interpreted to correspond to the Johnny Hoe suture), east-dipping reflections Su1 and Su2 (interpreted to correspond to delaminating crust of the Fort Simpson terrane), irregular reflection HC4 (interpreted to form the top of the Hottah crust), and east-dipping reflection HC5 (interpreted

© 2005 NRC Canada

to correspond to a dormant trench). The conductor is spatially correlated with the tectonic wedge, labelled TW in Fig. 13.

Solid silicate minerals are very resistive (>10^5 Ω·m at typical crustal conditions), so the interpreted sources of enhanced conductivity (i.e., decreased resistivity) involve minor geological constituents. There are four main mechanisms proposed to explain the enhanced conductivity in continental crust. These are enhanced ionic conduction in either aqueous fluids or partial melt or enhanced electronic conduction in either grain-boundary films of carbon or interconnected grains of graphite, sulphide, and metallic oxides (e.g., Jones 1992). In the case of the present survey, it is possible to exclude the first two possibilities. Studies have shown that fluid residence times in the crust are relatively short (e.g., Bailey 1990), and it is not feasible for the volumes of aqueous fluids required to explain the observed conductors to have persisted since the Proterozoic. Heat flow across the Wopmay Orogen along the Lithoprobe profile is higher than is typical for a Proterozoic terrane and averages 93 mW/m^2 (Majorowicz 1996; Hyndman et al. 2000; Lewis and Hyndman 2001). There is no evidence to suggest the presence of partial melt within the crust, however. Therefore, the source of the observed resistivity anomaly is interpreted to be caused by enhanced electronic conduction in grain-boundary films of carbon and (or) interconnected graphite, sulphide, or metallic grains.

MT studies have identified numerous crustal suture zones that exhibit enhanced electrical conductivity, and Boerner et al. (1996) review several examples of conductive Proterozoic sutures from North America. In many cases, the enhanced conductivity is related to the presence of oceanic rocks. Boerner et al. attribute the Proterozoic anomalies they examined to the presence of graphitic rocks formed when carbonaceous sedimentary rocks formed in pre-foredeep sequences are subsequently deformed and metamorphosed in a fold and thrust belt. An alternative explanation for Proterozoic conductors is provided by studies of the North American Central Plains conductor, which lies within the Proterozoic Trans-Hudson Orogen (e.g., Jones and Craven 1990; Jones et al. 1993). Jones et al. (1997) have shown that the conductor can be attributed to sulphides deposited in a hiatus in volcanism as the first of the island arcs of the La Ronge arc collides with the Rae–Hearn craton.

One interpretation of the Fort Simpson – Hottah conductor is that it is caused by the presence of metamorphosed oceanic rocks accreted during the early stages of the collisions between these terranes. The seismic reflection data provide evidence of imbricated subducted oceanic crust on the underside of the Hottah wedge (Cook et al. 1999) that could contribute to the observed resistivity anomaly. The MT method provides sufficient resolution of the geometry of the conductor, however, to indicate that it cannot be explained solely by rocks on the underside of the Hottah wedge. To explain the observed depth of the top of the anomaly, it is necessary for there to be conductive rocks either in the lower part of the Fort Simpson continental crust that was thrust over the Hottah wedge or in the Hottah wedge itself.

Based on the observed geometry of the conductor, the most likely interpretation of its source is that it is associated with Hottah rocks that were deformed and metamorphosed during collision. It is possible that fluids released from the subducting oceanic crust have contributed to the anomaly in the overlying continental crust. Deformation and metamorphism of ocean lithosphere containing a fluid phase can disperse carbon (Mareschal et al. 1992), and enhanced conductivity is observed in continental crust above presently actively subducting plates such as above the Juan de Fuca plate in Oregon, Washington, and southern British Columbia (Wannamaker et al. 1989; Kurtz et al. 1990; see also Jones 1993). In SNORCLE corridors 2 and 3 in the northern Cordillera (Yukon and northern British Columbia), a conductive anomaly is observed in a region in which subduction ceased at 40 Ma and is, therefore, attributed to a mineralogical constituent created by the subduction process rather than remnant fluid or thermal sources (Wennberg et al. 2002; Ledo et al. 2003). It is of note that the deformation associated with the Fort Simpson – Hottah collision involved significant fluid movement and subsequent melting of continental crust as indicated by the presence of calc-alkaline magmatism in the Fort Simpson magmatic arc.

The results of the GB tensor analysis provide further support for the interpretation of the conductor as a feature of the Fort Simpson – Hottah margin. The MT strike analysis suggests the dominant geoelectric strike direction in the upper crust is N30°E, which is oblique to the north–south margin between the Fort Simpson and Hottah terranes. We postulate that the conductor consists of a body with a large-scale trend parallel to the terrane margin but with localized translation of crustal blocks in the northeast–southwest direction. Such a conductor would create a three-dimensional response. Examination of the GB shear and twist values, which provide a measure of the three-dimensionality, confirms the values are higher than in adjacent areas at periods of >10 s in an area centred on site sno130. Although this GB analysis adds confidence to the interpretation of the source of the conductor, the presence of the 3-D response means that the 2-D models will provide a poorer representation of its detailed structure.

Coronation margin (?) and Hay River terrane conductor

The top of the conductive zone located beneath the surface boundary of the Hottah terrane and Great Bear magmatic arc (E in Fig. 10) is located at a depth of 10–20 km, and the zone extends around 40 km east beneath the magmatic arc. Seismic reflection results show that the Great Bear magmatic arc forms a relatively thin (~5 km) surface feature overlying deformed rocks of the Hottah–Slave transition, either from the Hottah terrane or correlative rocks of the Coronation margin (Cook et al. 1999). The observation of a conductor within the Coronation rocks to the north (Camfield et al. 1989) provides support to the interpretation of the rocks beneath the Great Bear magmatic arc as correlatives of the Coronation margin. In this case, following the reinterpretation of the Camfield et al. (1989) data by Boerner et al. (1996), the enhanced conductivity is attributed to graphitic or sulphidic rocks originally deposited in a restricted oceanic environment and subsequently metamorphosed and deformed during the final stages of the Calderan orogeny at around 1.8 Ma. The increased uranium concentration expected in such rocks may also contribute to the relatively high heat flow in the vicinity of the crustal conductor (Fig. 14).

The exact location at which the 1.86–1.74 Ga McDonald

© 2005 NRC Canada

Fig. 14. Comparison of heat flow data and concatenated 2-D resistivity models for corridors 1 and 1a. The heat flow is estimated from a contour map of the heat flow in northeast British Columbia and adjacent Northwest Territories in Majorowicz (1996). The site locations for the heat flow profile are projected onto an east–west line. The different projections of site locations on this profile and in the 2-D resistivity model cause the observed differences in the intersite spacing. Abbreviations as in Fig. 1.

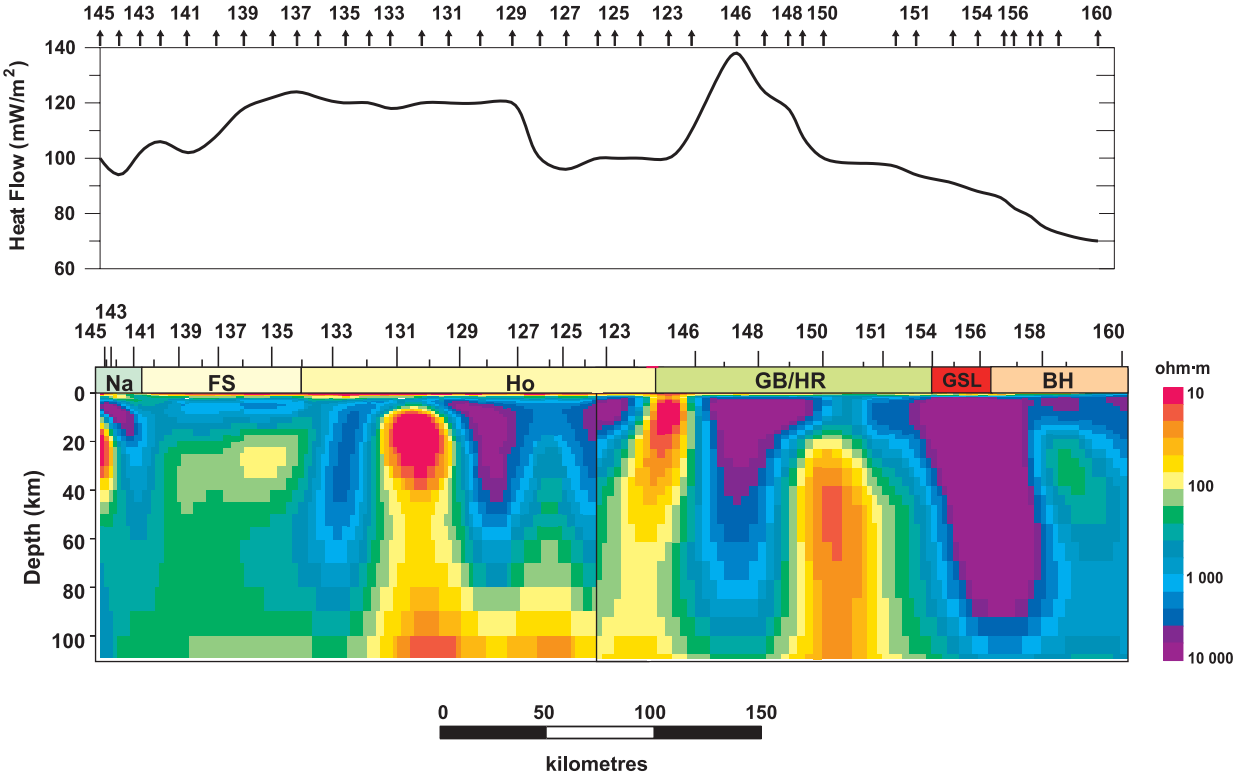

fault crosses corridor 1a is not known, but on the basis of potential-field truncations both Hildebrand et al. (1987) and Eaton and Hope (2003) place the fault at the location shown in Fig. 2. This location is between sites sno146 and sno148. Examination of Fig. 10 shows that the eastern margin of the crustal conductor is near site sno146. The resistivity model is consistent with the McDonald fault forming the eastern margin of the conductor, and the MT results therefore provide additional support for the proposed location of the fault.

Interpretation of the conductor located farther to the east in corridor 1a (labelled F in Fig. 10) is made difficult due to the uncertainty with which the tectonic elements are defined in the area to the north of the GSLsz and to the south of Great Slave Lake. In this area the Precambrian rocks are covered by ~600 m of Phanerozoic sedimentary rocks, and there are no crustal seismic reflection data.

Hottah mantle conductor

Enhanced conductivity is observed in the mantle beneath the Hottah terrane (labelled I in Fig. 10). The top of the conductive zone is at a depth of 60–80 km. The zone is spatially correlated with a number of seismic features and on this basis is interpreted to be caused by modification of the mantle associated with subduction during the collision and accretion of the Hottah terrane to the western margin of the Slave craton between 1.9 and 1.8 Ga and subsequent collision of the Fort Simpson terrane after 1.8 Ga. Seismic reflection results show delamination structures extending to 100 km depth in the mantle beneath the Great Bear magmatic arc, providing evidence that lower crustal Hottah rocks were emplaced in the mantle during subduction (Cook et al. 1998, 1999). Seismic refraction results (Fig. 13) show an anomalous mantle response in which at depths less than 60 km the velocity is about 7.7 km/s beneath the Hottah terrane, which is around 0.5 km/s lower than that in the adjacent areas (Fernández Viejo et al. 1999; Fernández Viejo and Clowes 2003). The anomaly, which extends to around 75 km depth, is interpreted by Fernández Viejo and Clowes (2003) as being caused by serpentinization of mantle peridotite by water derived from a subducting slab. Lastly, a mantle reflector resolved in seismic refraction studies (labelled J in Fig. 13), speculated to have a petrological origin (Fernández Viejo et al. 1999; Fernández Viejo and Clowes 2003), extends laterally along the top of the main part of the conductor.

Laboratory measurements on olivine at appropriate pressure–temperature mantle conditions indicate very high electrical resistivity values of >100 000 Ω·m (Constable and Duba 1990). Proposed sources of enhanced conductivity in the mantle differ from those proposed for the crust and include partial melt, a free aqueous fluid phase (Mibe et al. 1998), hydrogen dissolved in olivine (Karato 1990; Hirth et al. 2000), carbon-bearing material (Roberts et al. 1999), and sulphides (Ducea and Park 2000). We now examine the possibility that these mechanisms cause the Hottah conductor.

Geological evidence indicates that water was introduced into the mantle beneath the Hottah terrane through subduction: the calc-alkaline magmatism in the Great bear magmatic arc indicates that the mantle was hydrated at the time of the Fort

© 2005 NRC Canada

Simpson collision. It is significant that the depth of the shallow parts of the conductor (~60 km) correlates with the minimum depth at which free H_2O would become interconnected, according to dihedral wetting angle arguments (Mibe et al. 1998). It seems improbable, however, that free water could have persisted in the mantle over the 1.8 Ga since the end of subduction.

The seismic velocity anomaly is interpreted in terms of the presence of minerals hydrated during the subduction process, so it is appealing to interpret the overlapping resistivity anomaly in terms of either hydrous minerals or hydration of nominally anhydrous minerals. The coincidence of seismic reflection J with the top of the main part of the conductor provides support for the hypothesis that the decreased resistivity may be associated with a petrological change in the mantle. Boerner et al. (1999) proposed that hydrous mantle minerals, such as phlogopite, generated by metasomatising events, may explain enhanced mantle conductivity. However, other evidence does not support this hypothesis. Hydrous minerals in the crust do not enhance conductivity (Olhoeft 1981), and the region of North America that has experienced the highest amount of mantle metasomatism, around Baker Lake in the western Churchill Province of Canada, exhibits highly resistive mantle (Jones et al. 2002).

Heat flow is high across the Wopmay Orogen, exceeding 100 mW/m^2 along much of the Lithoprobe transect (Majorowicz 1996; Majorowicz et al. 2005; Hyndman et al. 2000; Lewis and Hyndman 2001). An alternative explanation for the Hottah mantle conductor is that it is due to partial melt associated with an upwarping of the asthenosphere. Figure 14 compares the measured heat flow with the MT resistivity model along the study transect. The observed variations in heat flow are representative of relatively large scale features extending tens of kilometres to the north and south. The results in Fig. 14 indicate a relatively low correlation at 10–100 km spatial scale between heat flow and mantle resistivity. For example, part of the Hottah mantle conductor between sno127 and sno123 is associated with a low in the heat-flow data. A zone of high heat flow (>115 mW/m^2) between sites sno129 and sno139 does not correlate with enhanced conductivity in the mantle and is associated with relatively high mantle seismic velocities (Fig. 13). The low correlation between the heat flow, enhanced mantle resistivity, and anomalous seismic velocities suggests the Hottah conductor is not caused by shallowing of the asthenosphere and the presence of partial melt.

After consideration of alternative hypotheses, the most probable cause of the Hottah conductor is carbon and (or) sulphides that were introduced into the mantle in sediments during subduction. Such materials could have been introduced in carbonaceous or sulphidic sediments subducted with underlying oceanic crust. The presence of a relatively small volume of either carbon or sulphides will produce a significant decrease in mantle resistivity (Roberts et al. 1999; Ducea and Park 2000). This interpretation is supported by the relatively low resistivities (<10 Ω·m) observed in the Hottah conductor.

Discussion of mantle strike azimuth

The strike azimuths observed at mantle depths in the Wopmay Orogen require comparison with several other datasets. Two-dimensionality at mantle depths is strongest in the Wopmay Orogen in the Nahanni terrane (between sites sno141 and sno145) and in the eastern Hottah terrane (sites sno123–sno129). Weaker two-dimensionality in the mantle beneath the Fort Simpson terrane and western Hottah terrane (sites sno129–sno140) occurs in a region interpreted to have been affected by extensional processes occurring during the formation of the Fort Simpson basin.

It is improbable that MT strike azimuths in the Wopmay Orogen are influenced significantly by known conductors outside the study area. The survey line is located 200 km north of the Kiskatinaw Conductor in northern Alberta (Boerner et al. 2000) and more than 300 km from a region of enhanced mantle conductivity in the central Slave craton (Jones et al. 2003, 2005). Conductors located at these distances from the survey sites will have minimal effect on the MT response at the depths of less than 120 km considered in this study. The Northern Wopmay Conductor detected by Camfield et al. (1989) in the exposed Coronation margin is located 500 km north of the present survey profile. It is possible that this conductor extends southwards into the study area and corresponds to the conductor observed beneath the western Great Bear magmatic arc. Considering the distribution of the MT strike directions and level of two-dimensionality across the Wopmay Orogen, however, it is unlikely that this crustal feature is significantly affecting the mantle responses.

The geological interpretation of deep MT and seismic strike results from northwestern Canada is complicated by the fact that many tectonic elements strike in a northeast direction, for example, both the GSLsz and the MF have a similar strike. It is impossible to exclude contributions to the mantle strike directions in the southeast of the present study area from the convergence of the Hottah terrane and Slave craton or from the earlier convergence of the Slave craton and Rae province which produced movement on the MF and GSLsz.

In a detailed study of sites near the GSLsz, Wu et al. (2001) defined a rotation in the strike angle, from ~N32°E at 10 s period to ~N65°E at >100 s period. Wu et al. interpreted the longer period strike angle observed near the GSLsz to be associated with the large-scale trend of the fault. If this explanation is correct, the deeper geoelectric structure was formed during the convergence and collision between the Archean Slave and Rae provinces between 2.03 and 1.95 Ga. In an examination of the observed seismic anisotropy near the GSLsz, Eaton and Hope (2003) found that an extensive region of the mantle surrounding the shear zone possesses an anisotropy with an axis parallel to the longer period MT strike direction.

Although structures associated with the GSLsz provide an explanation for the observed seismic anisotropy and long-period MT responses in the vicinity of the GSLsz, and possibly in the older Slave craton lithosphere to the north, they cannot explain the observation of similar MT strike directions throughout all of the (presumably?) younger lithosphere of the Wopmay Orogen.

In a number of recent studies (Simpson 2001; Bahr and Simpson 2002), long-period MT strike directions have been attributed to crystalline anisotropy formed at the base of the lithosphere by the present-day plate motion. The present-day absolute plate motion in the area of the Wopmay Orogen is

© 2005 NRC Canada

$\phi_{apm} \approx 54°$ (Minster and Jordan 1978). The observed strike direction at 120 km depth in the east of the study area is N62°E, which is reasonably consistent with the direction of plate motion, suggesting that the strike directions may be related to shearing of the subcontinental lithosphere. The change in the mantle strike angle in the west of the study area (Fig. 5) suggests either a thicker lithosphere in that area or a more dominant effect of fossil structures in the lithosphere, presumably associated with the formation of the Fort Simpson basin.

Conclusions

The magnetotelluric (MT) data collected along corridors 1 and 1a of the Lithoprobe SNORCLE transect have imaged a number of significant resistivity structures in the Wopmay Orogen and adjacent terranes. MT responses at periods less than 0.1 s to 1 s are controlled dominantly by the resistivity structure of the Phanerozoic rocks, which have an approximately 1-D structure. The MT responses at intermediate periods (1–100 s) indicate that the geoelectric strikes at crustal levels cluster around an azimuth of N30°E. These strikes are interpreted to be associated with pervasive transcurrent faulting interpreted to have formed during post-Calderan collision of the Fort Simpson terrane and (or) the Nahanni terrane with the Hottah terrane and Slave craton to the east. Comparison of the geometry of a conductor imaged at the boundary of the Fort Simpson and Hottah terranes with seismic reflection data suggests that the conductor is located within a west-pointing wedge of Hottah crust. A second conductor interpreted beneath the Great Bear magmatic arc provides some support for the interpretation of the existence of Coronation margin sediments near the southern extent of the Slave craton.

At mantle depths, the geoelectric strike in the eastern Wopmay Orogen rotates clockwise to an azimuth of around N40°E at ~70 km depth and then to N62°E at 120 km depth. The strike angle observed in the uppermost mantle is interpreted to reflect deformation formed with some coupling between the mantle and the crust linking ductile mantle deformation to the transcurrent faulting observed at the surface. The observed strike angles are most consistent with a transpressional collision of the Nahanni terrane with the western margin of the Wopmay Orogen. Further evidence of the Proterozoic modification of mantle resistivity structure comes in the observation of anomalously low resistivity in the Hottah mantle. The enhanced conductivity is interpreted to be related to the introduction of carbonaceous or sulphidic rocks into the mantle during the subduction of oceanic crust prior to the terminal Hottah–Slave and Fort Simpson – Hottah collisions. The clockwise rotation of strike at greater depth in the mantle is possibly due to present-day shearing at the base of the subcontinental lithosphere.

Geoelectric strike in the Fort Simpson terrane differs from that in the adjacent Nahanni and Hottah terranes. At crustal depths the structure is closer to 1-D than in the surrounding terranes, which are interpreted to be related to the Proterozoic sedimentary rocks within the Fort Simpson basin. At mantle depths the strike in the Fort Simpson terrane lies closer to north–south and is interpreted to reflect structures associated with the rifting event that produced the basin.

The Wopmay Orogen is a poorly exposed Proterozoic orogen that is completely covered in the southern and western parts by Phanerozoic sedimentary rocks. Geophysical investigations have provided considerable information on the orogen, allowing the definition of crustal and upper mantle structures produced by episodes of terrane collision, subduction, and accretion. MT results have contributed new information to these studies, e.g., defining a significant northeast–southwest crustal fabric extending beneath the covered part of the orogen into the Nahanni terrane. The MT results have also defined a northeast–southwest fabric in the upper mantle and delineated a localized zone of weaker two-dimensionality beneath the Fort Simpson basin. MT studies have also provided information complementary to that from other methods, e.g., providing support for the presence of Coronation margin sedimentary rocks or correlatives beneath the Great Bear magmatic arc and providing increased evidence for the presence of components derived from the crust in the mantle beneath the Hottah terrane.

Acknowledgments

Financial support for this project came from Lithoprobe, the Geological Survey of Canada, and the Natural Sciences and Engineering Research Council of Canada. Long-period MT data were collected with the assistance of Mr. N. Grant, Dr. C. Farquharson, Mr. B. Roberts, and Dr. I. Shiozaki using LiMS (long-period magnetotelluric system) instruments belong to the Geological Survey of Canada. Audio-frequency and broadband MT data were collected by Phoenix Geophysics, Toronto, Ontario. We would like to thank Dr. R. Mackie for advice on the use of his 2-D inversion program, Dr W. Brisbin for discussions concerning the tectonic structures of the Wopmay Orogen, and Dr. J. Majorowicz for providing information on the heat flow across the orogen. Reviews by M. Chouteau, M. Unsworth, and R. Clowes led to significant improvement of the manuscript.

References

Aitken, J.D. 1993. Cambrian and lower Ordovician – Sauk sequence. *In* Sedimentary cover of the craton in Canada. *Edited by* D.F. Stott and J.D. Aitken. Geological Survey of Canada, Geology of Canada, no. 5, pp. 96–124.

Aspler, L.B., Pilkington, M., and Miles, W.F. 2003. Interpretations of Precambrian basement based on recent aeromagnetic data, Mackenzie Valley, Northwest Territories. Geological Survey of Canada, Current Research 2003-C2.

Bahr, K., and Simpson, F. 2002. Electrical anisotropy below slow- and fast-moving plates: paleoflow in the upper mantle? Science (Washington, D.C.), **295**: 1270–1272.

Bailey, R.C. 1990. Trapping of aqueous fluids in the deep crust. Geophysical Research Letters, **17**: 1129–1132.

Bailey, R.C., and Groom, R.W. 1987. Decomposition of the magnetotelluric impedance tensor which is useful in the presence of channeling. *In* Expanded Abstracts of the 57th Annual International Society of Exploration Geophysicists Meeting and Exposition, Tulsa, Okla, pp. 154–156.

Bleeker, W., Ketchum, J.W.F., Jackson, V.A., and Villeneuve, M.E. 1999*a*. The Central Slave Basement Complex, Part I: its structural topology and autochthonous cover. Canadian Journal of Earth Sciences, **36**: 1083–1109.

© 2005 NRC Canada

Bleeker, W., Ketchum, J.W.F., and Davis, W.J. 1999*b*. The Central Slave Basement Complex, Part II: age and tectonic significance of high-strain zones along the basement–cover contact. Canadian Journal of Earth Sciences, **36**: 1111–1130.

Boerner, D., Kurtz, R., and Craven, J.A. 1996. Electrical conductivity and Paleo-Proterozoic foredeeps. Journal of Geophysical Research, **101**: 13 775 – 13 791.

Boerner, D.E., Kurtz, R.D., Craven, J.A., Ross, G.M., Jones, F.W., and Davis, W.J. 1999. Electrical conductivity in the Precambrian lithosphere of Western Canada. Science (Washington, D.C.,), **283**: 668–670.

Boerner, D.E., Kurtz, R.D., Craven, J.A., Ross, G.M., and Jones, F.W. 2000. A synthesis of electromagnetic studies in the Lithoprobe Alberta Basement Transect: constraints on Paleoproterozoic indentation tectonics. Canadian Journal of Earth Sciences, **37**: 1509–1534.

Bostick, F.X. 1977. A simple almost exact method of MT analysis. *In* Workshop on electrical methods in geothermal exploration. US. Geological Survey, Contract 14080001-8-359.

Camfield, P.A., Gupta, J.C., Jones, A.G., Kurtz, R.D., Krentz, D.H., Ostrowski, J.A., and Craven, J.A. 1989. Electromagnetic sounding and crustal electrical conductivity in the region of the Wopmay Orogen, Northwest Territories, Canada. Canadian Journal of Earth Sciences, **26**: 2385–2395.

Chave, A.D., and Thomson, D.J. 1989. Some comments on magnetotelluric response function estimation. Journal of Geophysical Research, **94**: 14 215 – 14 225.

Chave, A.D., Thomson, D.J., and Ander, M.E. 1987. On the robust estimation of power spectra, coherences, and transfer functions. Journal of Geophysical Research, **92**: 633–648.

Clowes, R.M. (*Editor*). 1997. Lithoprobe Phase V proposal — evolution of a continent revealed. Lithoprobe Secretariat, The University of British Columbia, Vancouver, B.C.

Constable, S.C., and Duba, A. 1990. Electrical conductivity of olivine, a dunite, and the mantle. Journal of Geophysical Research, **95**: 6967–6978.

Cook, F.A., van der Velden, A.J., Hall, K.W., and Roberts, B.J. 1998. Tectonic delamination and subcrustal imbrication of the Precambrian lithosphere in northwestern Canada mapped by Lithoprobe. Geology, **26**: 839–842.

Cook, F.A., van der Velden, A.J., Hall, K.W., and Roberts, B.J. 1999. Frozen subduction in Canada's Northwest Territories: Lithoprobe deep lithospheric reflection profiling of the western Canadian Shield. Tectonics, **18**: 1–24.

Cook, F.A., Clowes, R.M., Snyder, D.B., van der Velden, A.J., Hall, K.W., Erdmer, P., and Evenchick, C. 2004. Precambrian crust beneath the Mesozoic northern Canadian Cordillera discovered by Lithoprobe seismic reflection profiling. Tectonics, **23**: TC2010, doi:10.1029/2002TC001412.

deGroot-Hedlin, C., and Constable, S. 1990. Occam's inversion to generate smooth, two-dimensional models from magnetotelluric data. Geophysics, **55**: 1613–1624.

Douglas, R.J.W. 1973. Geology, Trout River, District of Mackenzie, Northwest Territories. Geological Survey of Canada, Map 1371A, scale 1 : 500 000.

Ducea, M.N., and Park, S.K. 2000. Enhanced mantle conductivity from sulfide minerals, southern Sierra Nevada, California. Geophysical Research Letters, **27**: 2405–2408.

Eaton, D.E., and Hope, J. 2003. Structure of the crust and upper mantle of the Great Slave Lake shear zone, northwestern Canada, from teleseismic analysis and gravity modelling. Canadian Journal of Earth Sciences, **40**: 1203–1218.

Eaton, D.W., Jones, A.G., and Ferguson, I.J. 2004. Lithospheric anisotropy structure inferred from collocated teleseismic and magnetotelluric observations: Great Slave Lake shear zone, northern Canada. Geophysical Research Letters, **31**: doi:10.1029/2004GRL020939.

Fernández Viejo, G., and Clowes, R.M. 2003. Lithospheric structure beneath the Archaean Slave Province and Proterozoic Wopmay orogen, northwestern Canada, from a Lithoprobe refraction/wide-angle reflection survey. Geophysical Journal International, **153**: 1–19.

Fernández Viejo, G., Clowes, R.M., and Amor, J.R. 1999. Imaging the lithospheric mantle in northwestern Canada with seismic wide-angle reflections. Geophysical Research Letters, **26**: 2809–2812.

Fischer, G., Schnegg, P., and Peguiron, M. 1981. An analytic one-dimensional magnetotelluric inversion scheme. Geophysical Journal of the Royal Astronomical Society, **67**: 257–278.

Garcia, X., and Jones, A.G. 2002. Atmospheric sources for audio-magnetotelluric (AMT) sounding. Geophysics, **67**: 448–458.

Garcia, X., Chave, A.D., and Jones, A.G. 1997. Robust processing of magnetotelluric data from the auroral zone. Journal of Geomagnetism and Geoelectricity, **49**: 1451–1468.

Groom, R.W., and Bailey, R.C. 1989. Decomposition of magnetotelluric impedance tensors in the presence of local three-dimensional galvanic distortion. Journal of Geophysical Research, **94**: 1913–1925.

Groom, R.W., and Bailey, R.C. 1991. Analytical investigations of the effects of near-surface three-dimensional galvanic scatterers on MT tensor decomposition. Geophysics, **56**: 496–518.

Groom, R.W., Kurtz, R.D., Jones, A.G., and Boerner, D.E. 1993. A quantitative methodology to extract regional magnetotelluric impedances and determine the dimension of the conductivity structure. Geophysical Journal International, **115**: 1095–1118.

Gupta, J.C., and Jones, A.G. 1990. Electrical resistivity structure of the Flathead Basin in southeastern British Columbia, Canada. Canadian Journal of Earth Sciences, **27**: 1061–1073.

Hanmer, S. 1988. Great Slave Lake shear zone, Canadian shield: reconstructed vertical profile of a crustal-scale fault zone. Tectonophysics, **149**: 245–264.

Hanmer, S., Bowring, S., Breemen, O., and Parrish, R. 1992. Great Slave Lake shear zone, NW Canada: mylonitic record of early Proterozoic continental convergence, collision and indentation. Journal of Structural Geology, **14**: 757–773.

Hildebrand, R.S., Hoffman, P.F., and Bowring, S.A. 1987. Tectonomagmatic evolution of the 1.9-Ga Great Bear magmatic zone, Wopmay orogen, northwestern Canada. Journal of Volcanology and Geothermal Research, **32**: 99–118.

Hirth, G., Evans, R.L., and Chave, A.D. 2000. Comparison of continental and oceanic mantle electrical conductivity: Is the Archean lithosphere dry? Geochemistry, Geophysics, Geosystems, **1**(Article): 2000GC000048.

Hoffman, P.F. 1987. Continental transform tectonics: Great Slave Lake shear zone (1.9 Ga), northwest Canada. Geology, **15**: 785–788.

Hoffman, P.F. 1989. Precambrian geology and tectonic history of North America. *In* The geology of North America — an overview. *Edited by* A.W. Bally and A.R. Palmer. Geological Society of America, The Geology of North America, Vol. A, pp. 447–512.

Hoffman, P.F., and Bowring, S.A. 1984. Short-lived 1.9 Ga continental margin and its destruction, Wopmay orogen, northwest Canada. Geology, **12**: 68–72.

Housh, T.B., and Bowring, S.A. 1988. Pb isotopic constraints on arc magmatism, Wopmay Orogen, NWT, Canada. EOS, **69**: 1510.

Hyndman, R.D., Lewis, T., and Flueck, P. 2000. The thermal regime of the SNORCLE Lithoprobe Transect and tectonic consequences. *In* Slave – Northern Cordillera Lithospheric Evolu-

© 2005 NRC Canada

tion (SNORCLE) Transect and Cordilleran Tectonics Workshop Meeting, Calgary, Alta., 25–27 February 2000. *Edited by* F.A. Cook and P. Erdmer. Lithoprobe Secretariat, The University of British Columbia, Vancouver, B.C., Lithoprobe Report 72, pp. 81–84.

Jones, A.G. 1980. Geomagnetic induction studies in Scandinavia — I. Determination of the inductive response function from the magnetometer array data. Journal of Geophysics, **48**: 181–194.

Jones, A.G. 1983*a*. On the equivalence of the "Niblett" and "Bostick" transformations in the magnetotelluric method. Zeitschrift für Geophysik, **53**: 72–73.

Jones, A.G. 1983*b*. The problem of "current channelling": a critical review. Geophysical Surveys, **6**: 79–122.

Jones, A.G. 1986. Parkinson's pointers' potential perfidy. Geophysical Journal of the Royal Astronomical Society, **87**: 1215–1224.

Jones, A.G. 1988. Static shift of magnetotelluric data and its removal in a sedimentary basin environment. Geophysics, **53**: 967–978.

Jones, A.G. 1992. Electrical conductivity of the lower continental crust. *In* Continental lower crust. *Edited by* D. Fountain, R.J. Arculus, and R.W. Kay. Elsevier, Amsterdam, The Netherlands, pp. 81–143.

Jones, A.G. 1993. Electromagnetic images of modern and ancient subduction zones. Tectonophysics, **219**: 29–45.

Jones, A.G. 1999. Imaging the continental upper mantle using electromagnetic methods. Lithos, **48**: 57–80.

Jones, A.G., and Craven, J.A. 1990. The North American Central Plains conductivity anomaly and its correlation with gravity, magnetics, seismic and heat flow data in the Province of Saskatchewan. Physics of the Earth and Planetary Interiors, **60**: 169–194.

Jones, A.G., and Ferguson, I.J. 2001. The electric Moho. Nature (London), **409**: 331–333.

Jones, A.G., and Spratt, J. 2002. A simple method for deriving the uniform field MT responses in auroral zones. Earth, Planets and Space, **54**: 443–450.

Jones, A.G., Chave, A.D., Egbert, G., Auld, D., and Bahr, K. 1989. A comparison of techniques for magnetotelluric response function estimation. Journal of Geophysical Research, **94**: 14 201 – 14 213.

Jones, A.G., Craven, J.A., McNeice, G.W., Ferguson, I.J., Boyce, T.T., Farquharson, C., and Ellis, R. 1993. North American Central Plains conductivity anomaly within the Trans-Hudson orogen in northern Saskatchewan, Canada. Geology, **21**: 1027–1030.

Jones, A.G., Katsube, J., and Schwann, P. 1997. The longest conductivity anomaly in the world explained: sulphides in fold hinges causing very high electrical anisotropy. Journal of Geomagnetism and Geoelectricity, **49**: 1619–1629.

Jones, A.G., Ferguson, I.J., Chave, A., Evans, R., and McNeice, G. 2001. The electric lithosphere of the Slave Craton. Geology, **29**: 423–426.

Jones, A.G., Snyder, D., Hanmer, S., Asudeh, I., White, D., Eaton, D., and Clarke, G. 2002. Magnetotelluric and teleseismic study across the Snowbird Tectonic Zone, Canadian Shield: a Neoarchean mantle suture? Geophysical Research Letters, **29**: doi: 10.1029/2002GL015359.

Jones, A.G., Lezaeta, P., Ferguson, I.J., Chave, A.D., Evans, R.L., Garcia, X., and Spratt, J. 2003. The electrical structure of the Slave craton. Lithos, **71**: 505–527.

Jones, A.G., Ledo, J., Ferguson, I.J., Grant, N., McNeice, G., Spratt, J., Farquharson, C., Roberts, B., Wennberg, G., Wolynec, L., and Wu, X. 2005. A 1600 km-long magnetotelluric transect from the Archean to the Tertiary: SNORCLE MT overview. Canadian Journal of Earth Sciences, **42**: this issue.

Karato, S. 1990. The role of hydrogen in the electrical conductivity of upper mantle. Nature (London), **347**: 272–273.

Kurtz, R.D., DeLaurier, J.M., and Gupta, J.C. 1990. The electrical conductivity distribution beneath Vancouver Island: a region of active plate subduction. Journal of Geophysical Research, **95**: 10 929 – 10 946.

Law, J. 1971. Regional Devonian geology and oil and gas possibilities, upper Mackenzie River area. Bulletin of Canadian Petroleum Geology, **19**: 437–486.

Ledo, J., Jones, A.G., Ferguson, I.J., and Wolynec, L. 2003. Lithospheric structure of the Yukon, northern Canadian Cordillera, obtained from magnetotelluric data. Journal of Geophysical Research, **109**: B04410, doi: 10.1029/2003JB002516.

Lewis, T., and Hyndman, R.D. 2001. High heat flow and high crustal temperatures along the SNORCLE Transect. *In* Lithoprobe SNORCLE Transect and Cordilleran Tectonics Workshop, Sidney, B.C., 25–27 February 2001. Lithoprobe Secretariat, The University of British Columbia, Vancouver, B.C., Lithoprobe Report 79, pp. 28–29.

Majorowicz, J.A. 1996. Anomalous heat flow regime in the western margin of the North American Craton. Journal of Geodynamics, **21**: 123–140.

Majorowicz, J.A., Jessop, A.M., and Lane, L.S. 2005. Regional heat flow pattern and lithospheric geotherms in northeastern British Columbia and adjacent Northwest Territories, Canada. Canadian Society of Petroleum Geologists Bulletin, **53**: 51–66.

Mareschal, M., Fyfe, W.S., Percival, J., and Chan, T. 1992. Grain-boundary graphite in Kapuskasing gneisses and implication for lower-crustal conductivity. Nature (London), **357**: 674–676.

Marquis, G., Jones, A.G., and Hyndman, R.D. 1995. Coincident conductive and reflective lower crust across a thermal boundary in southern British Columbia, Canada. Geophysical Journal International, **120**: 111–131.

Meijer-Drees, N.C. 1975. Geology of the lower Paleozoic formations in the subsurface of the Fort Simpson area, district of Mackenzie, NWT. Geological Survey of Canada, Paper 74-40.

Mibe, K., Fujii, T., and Yasuda, A. 1998. Connectivity of aqueous fluid in the Earth's upper mantle. Geophysical Research Letters, **25**: 1233–1236.

Minster, J.B., and Jordan, T.H. 1978. Present-day plate motions. Journal of Geophysical Research, **83**: 5331–5354.

Niblett, E.R., and Sayn-Wittgenstein, C. 1960. Variation of the electrical conductivity with depth by the magnetotelluric method. Geophysics, **25**: 998–1008.

Olhoeft, G.R. 1981. Electrical properties of granite with implications for the lower crust. Journal of Geophysical Research, **86**: 931–936.

Parkinson, W.D. 1962. The influence of continents and oceans on geomagnetic variations. Geophysical Journal of the Royal Astronomical Society, **6**: 441–449.

Pilkington, M., Miles, W.F., Ross, G.M., and Roest, W.R. 2000. Potential-field signatures of buried Precambrian basement in the Western Canada Sedimentary Basin. Canadian Journal of Earth Sciences, **37**: 1453–1471.

Rhodes, D., Lantos, E.A., Lantos, J.A., Webb, R.J., and Owens, C. 1984. Pine Point orebodies and their relationship to the stratigraphy, structure, dolomitization, and karstification of the Middle Devonian Barrier Complex. Economic Geology, **79**: 991–1055.

Ritts, B.D., and Grotzinger, J.P. 1994. Depositional facies and detrital composition of the Paleoproterozoic Et-Then Group, N.W.T., Canada: sedimentary response to intracratonic indentation. Canadian Journal of Earth Sciences, **31**: 1763–1778.

Roberts, J.J., Duba, A.G., Mathez, E.A., Shankland, T.J., and Kinzler,

© 2005 NRC Canada

R. 1999. Carbon-enhanced electrical conductivity during fracture of rocks. Journal of Geophysical Research, **104**: 737–747.

Rodi, W., and Mackie, R.L. 2001. Nonlinear conjugate gradients algorithm for 2-D magnetotelluric inversion. Geophysics, **66**: 174–187.

Ross, G.M. 2002. Evolution of continental lithosphere in Western Canada: results from Lithoprobe studies in Alberta and beyond. Canadian Journal of Earth Sciences, **39**: 413–437.

Ross, G.M., Annell, H.C., and Hamilton, M.A. 2000. Lithology and U–Pb geochronology of shallow basement along the SNORCLE line, southwest Northwest Territories: a preliminary report. *In* Slave – Northern Cordillera Lithospheric Evolution (SNORCLE) Transect and Cordilleran Tectonics Workshop Meeting, Calgary, Alta., 25–27 February 2000. *Edited by* F.A. Cook and P. Erdmer. Lithoprobe Secretariat, The University of British Columbia, Vancouver, B.C., Lithoprobe Report 72, pp. 76–80.

Schmucker, U., and Janknowsky, J. 1972. Geomagnetic induction studies and the electrical state of the upper mantle. Tectonophysics, **13**: 233–256.

Simpson, F. 2001. Resistance to mantle flow inferred from the electromagnetic strike of the Australian upper mantle. Nature (London), **412**: 632–635.

Snyder, D.B. 2000. Wedge geometries in arc–continent convergence tectonics of the Wopmay, Svecofennian orogens and beyond. *In* Slave – Northern Cordillera Lithospheric Evolution (SNORCLE) Transect and Cordilleran Tectonics Workshop Meeting, Calgary, Alta., 25–27 February 2000. *Edited by* F.A. Cook and P. Erdmer. Lithoprobe Secretariat, The University of British Columbia, Vancouver, B.C., Lithoprobe Report 72, pp. 74–75.

Snyder, D.B., Clowes, R.M., Cook, F.A., Erdmer, P., Evenchik, C.A., van der Velden, A.J., and Hall, K.W. 2002. Proterozoic prism arrests suspect terranes: insights into the ancient cordilleran margin from seismic reflection data. GSA Today, **12**: 4–10.

Sternberg, B.K., Washburne, J.C., and Anderson, R.G. 1985. Investigation of MT static shift correction methods. *In* Expanded Abstracts of the 55th Annual International Society of Exploration Geophysicists Meeting and Exposition, Tulsa, Okla., pp. 264–267.

Swift, C.M. 1967. A magnetotelluric investigation of an electrical conductivity anomaly in the southwestern United States. Ph.D. thesis, Massachusetts Institute of Technology, Cambridge, Mass.

Villeneuve, M.E., Thériault, R.J., and Ross, G.M. 1991. U–Pb ages and Sm–Nd signature of two subsurface granites from the Fort Simpson magnetic high, northwest Canada. Canadian Journal of Earth Sciences, **28**: 1003–1008.

Vozoff, K. 1991. The magnetotelluric method. *In* Electromagnetic methods in applied geophysics. Vol. 2. Applications. *Edited by* M.N. Nabighian. Society of Exploration Geophysicists, Tulsa, Okla., pp. 641–711.

Wannamaker, P.E., Hohmann, G.W., and Ward, S.H. 1984. Magnetotelluric responses of three-dimensional bodies in layered earths. Geophysics, **49**: 1517–1533.

Wannamaker, P.E., Stodt, J.A., and Rijo, L. 1987. A stable finite element solution for two-dimensional magnetotelluric modelling. Geophysical Journal of the Royal Astronomical Society, **88**: 277–296.

Wannamaker, P.E., Booker, J.R., Jones, A.G., Chave, A.D., Filloux, J.H., Waff, H.S., and Law, L.K. 1989. Resistivity cross-section through the Juan de Fuca subduction system and its tectonic implications. Journal of Geophysical Research, **94**: 14 127 – 14 144.

Wennberg, G., Ferguson, I.J., Ledo, J., and Jones, A.G. 2002. Modeling and interpretation of magnetotelluric data: Watson Lake to Stewart (line 2A) and Johnsons's Crossing to Watson lake. *In* Proceedings of the 2002 SNORCLE Transect and Cordilleran Tectonics Workshop, Sidney, B.C., 21–24 February 2002. Lithoprobe Secretariat, The University of British Columbia, Vancouver, B.C., Lithoprobe Report 82, pp. 145–152.

Wheeler, J.O., Hoffman, P.F., Card, K.D., Davidson, A., Sanford, B.V., Okulitch, A.V., and Roest, W.R. 1997. Geological map of Canada. Geological Survey of Canada, Map 1860A.

Wu, X. 2001. Determination of near-surface, crustal and lithospheric structures in the Canadian Precambrian Shield using time-domain electromagnetic and magnetotelluric methods. Ph.D. thesis, University of Manitoba, Winnipeg, Man. 506 p.

Wu, X., Ferguson, I.J., and Jones, A.G. 2002. Magnetotelluric response and geoelectric structure of the Great Slave Lake Shear Zone. Earth and Planetary Science Letters, **196**: 35–50.

© 2005 NRC Canada